Microbiology and Immunology

Microbiol Immunol 2009; **53**: 417–420
doi:10.1111/j.1348-0421.2009.00133.x

NOTE

Distinct genotype and antigenicity among genogroup II sapoviruses

Tomoichiro Oka*, Kana Miyashita*, Kazuhiko Katayama, Takaji Wakita and Naokazu Takeda

Department of Virology II, National Institute of Infectious Diseases, Gakuen 4-7-1, Musashi-murayama, Tokyo 208-0011, Japan

ABSTRACT

SaV, a pathogen of acute gastroenteritis, is divided into five genogroups, GI to GV. However, the relation between SaV antigenicity and genetic clusters is not fully understood. We have recently identified two GII SaV strains, Mc10 and C12, which are grouped into the same cluster based on the polymerase but are grouped into distinct clusters based on the capsid. To evaluate the difference in antigenicity between these two strains, VLP were expressed in mammalian cells. An antigen ELISA demonstrated for the first time that strains in the same GII SaV genogroup, but within different clusters, have distinct antigenicities.

Key words antigenicity, sapovirus, virus-like particles

SaV, a member of the family *Caliciviridae*, is a pathogen of acute gastroenteritis and composed of many genetically distinct strains. SaV contains a single-stranded positive sense RNA genome of approximately 7.5 kb that is polyadenylated at its 3′ terminus. The SaV genomes are predicted to encode two or three ORF. The SaV ORF1 encodes non-structural proteins and a single structural protein (VP1), while the functions of the ORF2- and ORF3-encoded proteins are still unknown (1). In SaV, the icosahedral capsid is formed from a single gene product, VP1 (2), which is thought to be produced as the ORF1 polyprotein followed by cleavage with viral encoded protease, or translation from subgenomic RNA (3′-coterminal with the virus genome), or both (3–7). On the basis of the nucleotide sequence of the capsid, SaV strains are divided into five genogroups, GI, GII, GIII, GIV, and GV, and each genogroup is further subdivided into genotypes (1,8). The SaV GI, GII, GIV, and GV strains infect humans, while the GIII strains infect swine. At present, only the specific strains belonging to GIII are cultivable. The SaV Mc10 and C12 strains have been identified as "recombinant SaV strains," and they are grouped into the same cluster based on the polymerase, but into separate distinct clusters based on the capsid (9). In previous studies in which the expression of recombinant SaV VLP was performed with insect expression systems (10–14), formation of Mc10 VLP was not achieved (9), and production of C12 VLP was insufficient to prepare the antibody (10); therefore, the antigenicity of these two strains remains unknown. We have recently reported successful formation of SaV Mc10 VLP in COS-7 cells (3, 6). In addition, an increase in VLP yield was observed when a three-nucleotide sequence, "ACC", was added prior to the start codon of the putative SaV subgenomic RNA region in insect cells (14).

In this study, we have examined (i) whether efficient SaV C12 VLP formation could be achieved in a mammalian expression system; (ii) whether the SaV VLP yield in mammalian cells could be increased by the introduction of an additional nucleotide sequence prior to the start codon of the putative SaV subgenomic RNA region; and (iii) whether or not the antigenicity of the Mc10 and C12 strains is identical. To construct an Mc10 VLP expression plasmid with an additional "ACC" nucleotide sequence prior to the capsid start codon, site-directed mutagenesis

*These authors contributed equally to this study.

Correspondence
Tomoichiro Oka, Department of Virology II, National Institute of Infectious Diseases, Gakuen 4-7-1, Musashi-murayama, Tokyo 208-0011, Japan.
Tel: +81 42 561 0771; fax: +81 42 561 4729; email: oka-t@nih.go.jp

Received 21 January 2009; revised 2 March 2009; accepted 5 March 2009.

List of Abbreviations: Aa, amino acid; MAb, monoclonal antibody; MOI, multiplicity of infection; NoV, norovirus; OD, optical density; ORF, open reading frame; PBS-T, PBS containing 0.05% Tween 20; SaV, sapovirus; VLP, virus-like particles.

© 2009 The Societies and Blackwell Publishing Asia Pty Ltd

was performed with a sense primer, 5′-CTATAGGGAA CAGCCACC**ACC**ATGGAGGGCCTAGGCCAACCAC-3′, containing an additional "ACC" sequence (bold), and Mc10-specific sequence (underlined), and an antisense primer, 5′-GGTGGCTGTTCCCTATAGTGAGTC GTATTA-3′, using a GeneTailor Site Directed Mutagenesis Kit (Invitrogen, Tokyo, Japan) with the SaV Mc10 T7 capsid-genome end/pUC19 (3) as a template. The resulting plasmid was designated the SaV ACCMc10 T7 -capsid-genome end/pUC19. To construct the SaV C12 VLP expression plasmid, a DNA fragment corresponding to the putative capsid gene, ORF2 gene and untranslated region of the genome (nt 5173–7476: GenBank Accession No. AY603425) was amplified with a plasmid, pDONR201/ SaV C12 (10), which contains a putative C12 subgenomic region as the template. A sense primer, 5′-CCCTGggatcc**TAATACGACTCACTATA**GGGAACAGCC ACCATGGAGGGTGTACCCCGC-3′, containing a *Bam*HI site (lower case), the T7 promoter sequence (bold), and a C12-specific sequence (underlined), and an antisense primer, 5′-GTCCTagatctT_{29} CCTAGAATATGTGGCTGTGATCG-3′, containing the *Bgl*II site indicated (lower case) and a C12-specific sequence (underlined), were used. PCR was performed with KOD-Plus-DNA polymerase (Toyobo, Osaka, Japan), and then the PCR products were purified and cloned into pUC19 vector (Toyobo) as previously described (3). The resultant plasmid was designated SaV C12 T7 capsid-genome end/pUC19. To construct the C12 VLP expression plasmid with an additional "ACC" nucleotide sequence prior to the capsid start codon, site-directed mutagenesis was performed with a sense primer, 5′-CACTATAG GGAACAGCCACC**ACC**ATGGAGGGTGTACCCCC-3′, including the additional "ACC" sequence (bold), and C12-specific sequence (underlined), and an antisense primer, 5′-GGTGGCTGTTCCCTATAGTGAGTCGTATT AGGATCC-3′, as described above with SaV C12 T7 capsid-genome end/pUC19 as a template. The resulting plasmid was designated SaV ACCC12 capsid-genome end/pUC19. *Escherichia coli* DH5α cells (Toyobo) were used for transformation and propagation of the plasmid.

SaV VLP were expressed as previously described (3). In brief, COS-7 cells established from African green monkey kidney cells grown in 6-well culture plates (BD Falcon, Franklin Lakes, NJ, USA) were infected with a recombinant vaccinia virus which expresses the T7 RNA polymerase (15) at a MOI of 1, and incubated at 37°C for 1 hr. Then, the plasmids SaV Mc10 T7 capsid-genome end/pUC19, SaV ACCMc10 T7 capsid-genome end /pUC19, SaV C12 T7 capsid-genome end /pUC19, or SaV ACCC12 T7 capsid-genome end/pUC19, each at 1 μg per well, were transfected into COS-7 cells using Effectene Transfection Reagent (Qiagen, Valencia, CA, USA) according to the manufacturer's protocol. To purify the VLP, the cell suspension (collected from 20 six-well plates for each construct) was subjected to three cycles of freezing and thawing, and the cell debris was removed by centrifugation (2300 × *g* for 5 min at 4°C). VLP from the cell lysate were purified by ultracentrifugation as previously described (6). For large-scale VLP expression, 80 six-well plates were used and the process was repeated several times.

Hyperimmune sera against newly expressed Mc10 or C12 VLP were prepared in rabbits and guinea pigs as previously described (13). Immunization of rabbits was performed at Keari (Osaka, Japan), and immunization of guinea pigs was done at Japan-Lamb (Hiroshima, Japan).

Titration of hyperimmune sera was performed as previously described (13). An antigen ELISA was performed to examine the cross-reactivities of the VLP. One-hundred μl of a 1:4000 diluted hyperimmune rabbit antiserum containing ELISA titers of 1 024 000 against Mc10 or C12 VLP was used to coat a 96-well microtiter plate (Immulon 2HB; Thermo Electron Corporation, Waltham, MA, USA) by incubation at 4°C overnight. The wells were then blocked with 200 μl of PBS containing 5% skim milk (Becton Dickinson, Sparks, MD, USA) by incubation at 4°C overnight. After the plate had been washed four times with 350 μL of PBS-T, 100 μl of the VLP (100 ng) in PBS was added, and the plate was incubated for 3 hr at room temperature. After the plate had been washed five more times, 100 μl of a 1:16 000 dilution of hyperimmune guinea pig antiserum containing ELISA titers of 1:128 000 against Mc10 VLP or 100 μl of a 1:16 000 dilution of hyperimmune guinea pig antiserum containing ELISA titers of 1:4 096 000 against C12 VLP was added to each well, and the mixture was incubated for 1 hr at 37°C. After the plate had been washed four additional times, 100 μl of a 1:1000 dilution of horseradish peroxidase-conjugated rabbit anti-guinea pig immunoglobulin G (Cappel, West Chester, PA, USA) diluted in PBS-T was added, and the mixture was incubated for 1 hr at 37°C. After the plate had been washed, 100 μl of phosphate citrate buffer (pH 5.0, Sigma, St. Louis, MO, USA) containing 0.4 g/l *o*-phenylenediamine and 0.124 ml/l H_2O_2 was added to each well. After 30 min, the reaction was stopped by addition of 50 μL of 4N H_2SO_4. The absorbance was measured immediately at 492 nm by a microplate reader.

The Mc10 and C12 VLP were mostly found in cell lysate, which was purified by ultracentrifugation, as previously described (3). Approximately 80 μg of purified Mc10 and C12 VLP was obtained from COS-7 cells grown in 80 six-well plates, whereas 120 μg of the VLP was obtained when the Mc10 construct with the additional nucleotide sequence "ACC" was expressed. The additional nucleotide sequence "ACC" had no effect on the yield of C12 VLP

© 2009 The Societies and Blackwell Publishing Asia Pty Ltd

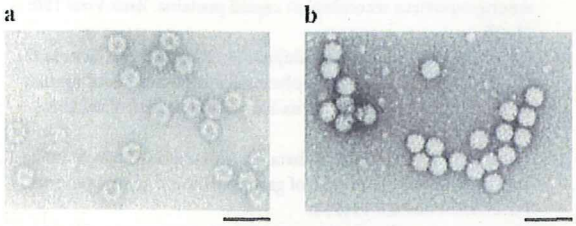

Fig. 1. Electron micrograph of purified (a) Mc10 VLP and (b) C12 VLP expressed in COS-7 cells. Purified VLP were stained with 4% uranyl acetate (pH 4) and examined with an electron microscope (JEM-1220; Jeol, Tokyo, Japan) operating at 80 kV. The bar indicates 100 nm.

(data not shown). The purified VLP were approximately 40–45 nm in diameter (Fig. 1). In this study, the cross-reactivities of SaV Mc10 and C12 VLP were analyzed by using antigen ELISA. The OD values at 492 nm against homologous VLP were similar; that is, 1.633 for Mc10 VLP, and 1.681 for C12 VLP. In contrast, the OD values against heterologous VLP were 0.251 for Mc10 VLP and 0.313 for C12 VLP.

As depicted in Figure 2, the C12 VLP and Mc10 VLP were clustered into different genotypes in the same genogroup, genogroup II. Our results demonstrate that the additional nucleotide sequence "ACC" prior to the VP1 start codon increases the yield of Mc10 VLP in a mammalian expression system by an unknown mechanism. Importantly, the degree of expression of the VLP was sufficient to prepare rabbit and guinea pig antisera to construct an antigen ELISA. The Mc10 and C12 VLP were antigenically distinct by the antigen ELISA, because the OD values were significantly different between homologous and heterologous VLP. Because no SaV-specific antibody was detected in the preimmune animal sera, and antibody against cell components was barely generated (data not shown), the low level of cross-reaction observed between these two strains indicates that antibodies which recognize common antigenic epitope(s) were generated. In fact, the amino acid identity between Mc10 VP1 (558 aa) and C12 VP1 (561 aa) is 79.1%. Although distinct antigenicity has been reported among SaV GI, GII, GIV, and GV VLP, and between two strains, Mc114 and Yokote1, in GI VLP (13), our results indicate the possibility of developing MAb either broadly reactive to all SaV genogroups or specifically reactive to individual SaV genogroups and/or genotypes, as has been shown for NoV (16, 17), a pathogen for human acute gastroenteritis belonging to the family *Caliciviridae*, which includes antigenically highly divergent strains (18, 19). ELISA and immunochromatography kits to detect NoV are commercially available.

In conclusion, this study demonstrates that two SaV strains, Mc10 and C12, belonging to different genotypes

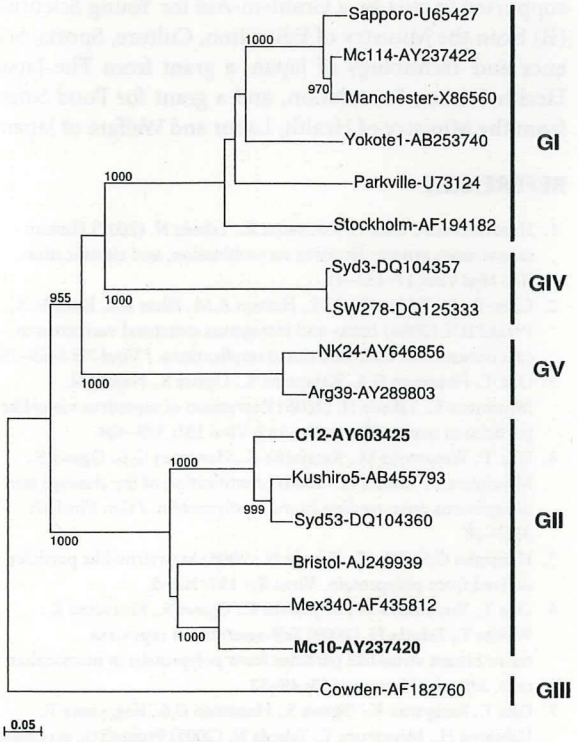

Fig. 2. Phylogenetic tree of SaV based on complete capsid nucleotide sequences (approx. 1700 nt). Nucleotide sequences were aligned with Clustal W version 1.83. (http://clustalw.ddbj.nig.ac.jp/top-j.html). A phylogenetic tree with 1000 bootstrap replications was constructed by the neighbor-joining method. The distance of nucleotide substitutions per site was calculated by Kimura's two-parameter method, and was illustrated with NJPlot software (http://pbil.univ-lyon1.fr/software/njplot.html). The number on each branch indicates the bootstrap value, and a value of 950 or higher is considered statistically significant for the grouping. The scale represents nucleotide substitutions per site.

within the same SaV GII have different antigenicity. The results in this study as well as those of previous studies (10–13) indicate that the antigenicity of SaV reflects the VP1-based genogrouping and genotyping of SaV well, although a common epitope(s) is likely to exist. Accumulation of SaV VLP panels may help to establish MAb either broadly or specifically reactive to SaV strains. The SaV VLP expression system using mammalian cells is similar to using insect cells and a useful tool for the preparation of VLP.

ACKNOWLEDGMENTS

We thank B. Moss for providing the recombinant vaccinia virus encoding T7 RNA polymerase and G. S. Hansman for his assistance in electron microscopy. This work was

© 2009 The Societies and Blackwell Publishing Asia Pty Ltd

supported in part by a Grant-in-Aid for Young Scientists (B) from the Ministry of Education, Culture, Sports, Science and Technology of Japan, a grant from The Japan Health Science Foundation, and a grant for Food Safety from the Ministry of Health, Labor and Welfare of Japan.

REFERENCES

1. Hansman G.S., Oka T., Katayama K., Takeda N. (2007) Human sapoviruses: genetic diversity, recombination, and classification. *Rev Med Virol* **17:** 133–41.
2. Chen R., Neill J.D., Noel J.S., Hutson A.M., Glass R.I., Estes M.K., Prasad B.V. (2004) Inter- and intragenus structural variations in caliciviruses and their functional implications. *J Virol* **78:** 6469–79.
3. Oka T., Hansman G.S., Katayama K., Ogawa S., Nagata N., Miyamura T., Takeda N. (2006) Expression of sapovirus virus-like particles in mammalian cells. *Arch Virol* **151:** 399–404.
4. Oka T., Yamamoto M., Katayama K., Hansman G.S., Ogawa S., Miyamura T., Takeda N. (2006) Identification of the cleavage sites of sapovirus open reading frame 1 polyprotein. *J Gen Virol* **87:** 3329–38.
5. Hansman G.S., Oka T., Takeda N. (2008) Sapovirus-like particles derived from polyprotein. *Virus Res* **137:** 261–5.
6. Oka T., Yamamoto M., Miyashita K., Ogawa S., Katayama K., Wakita T., Takeda N. (2009) Self-assembly of sapovirus recombinant virus-like particles from polyprotein in mammalian cells. *Microbiol Immunol* **53:** 49–52.
7. Oka T., Katayama K., Ogawa S., Hansman G.S., Kageyama T., Ushijima H., Miyamura T., Takeda N. (2005) Proteolytic processing of sapovirus ORF1 polyprotein. *J Virol* **79:** 7283–90.
8. Farkas T., Zhong W.M., Jing Y., Huang P.W., Espinosa S.M., Martinez N., Morrow A.L., Ruiz-Palacios G.M., Pickering L.K., Jiang X. (2004) Genetic diversity among sapoviruses. *Arch Virol* **149:** 1309–23.
9. Katayama K., Miyoshi T., Uchino K., Oka T., Tanaka T., Takeda N., Hansman G.S. (2004) Novel recombinant sapovirus. *Emerg Infect Dis* **10:** 1874–6.
10. Hansman G.S., Natori K., Oka T., Ogawa S., Tanaka K., Nagata N., Ushijima H., Takeda N., Katayama K. (2005) Cross-reactivity among sapovirus recombinant capsid proteins. *Arch Virol* **150:** 21–36.
11. Hansman G.S., Natori K., Ushijima H., Katayama K., Takeda N. (2005) Characterization of polyclonal antibodies raised against sapovirus genogroup five virus-like particles. *Arch Virol* **150:** 1433–7.
12. Hansman G.S., Saito H., Shibata C., Ishizuka S., Oseto M., Oka T., Takeda N. (2007) Outbreak of gastroenteritis due to sapovirus. *J Clin Microbiol* **45:** 1347–9.
13. Hansman G.S., Oka T., Sakon N., Takeda N. (2007) Antigenic diversity of human sapoviruses. *Emerg Infect Dis* **13:** 1519–25.
14. Hansman G.S., Oka T., Katayama K., Takeda N. (2006) Enhancement of sapovirus recombinant capsid protein expression in insect cells. *FEBS Lett* **580:** 4047–50.
15. Fuerst T.R., Niles E.G., Studier F.W., Moss B. (1986) Eukaryotic transient-expression system based on recombinant vaccinia virus that synthesizes bacteriophage T7 RNA polymerase. *Proc Natl Acad Sci U S A* **83:** 8122–6.
16. Kitamoto N., Tanaka T., Natori K., Takeda N., Nakata S., Jiang X., Estes M.K. (2002) Cross-reactivity among several recombinant calicivirus virus-like particles (VLPs) with monoclonal antibodies obtained from mice immunized orally with one type of VLP. *J Clin Microbiol* **40:** 2459–65.
17. Shiota T., Okame M., Takanashi S., Khamrin P., Takagi M., Satou K., Masuoka Y., Yagyu F., Shimizu Y., Kohno H., Mizuguchi M., Okitsu S., Ushijima H. (2007) Characterization of a broadly reactive monoclonal antibody against norovirus genogroups I and II: recognition of a novel conformational epitope. *J Virol* **81:** 12298–306.
18. Hansman G.S., Natori K., Shirato-Horikoshi H., Ogawa S., Oka T., Katayama K., Tanaka T., Miyoshi T., Sakae K., Kobayashi S., Shinohara M., Uchida K., Sakurai N., Shinozaki K., Okada M., Seto Y., Kamata K., Nagata N., Tanaka K., Miyamura T., Takeda N. (2006) Genetic and antigenic diversity among noroviruses. *J Gen Virol* **87:** 909–19.
19. Kamata K., Shinozaki K., Okada M., Seto Y., Kobayashi S., Sakae K., Oseto M., Natori K., Shirato-Horikoshi H., Katayama K., Tanaka T., Takeda N., Taniguchi K. (2005) Expression and antigenicity of virus-like particles of norovirus and their application for detection of noroviruses in stool samples. *J Med Virol* **76:** 129–36.

© 2009 The Societies and Blackwell Publishing Asia Pty Ltd

Virology 394 (2009) 119–129

Contents lists available at ScienceDirect

Virology

journal homepage: www.elsevier.com/locate/yviro

Structural and biological constraints on diversity of regions immediately upstream of cleavage sites in calicivirus precursor proteins

Tomoichiro Oka [a,*,1], Masaru Yokoyama [b,1], Kazuhiko Katayama [a], Hiroshi Tsunemitsu [c], Mami Yamamoto [a], Kana Miyashita [a], Satoko Ogawa [a,2], Kazushi Motomura [b], Hiromi Mori [b], Hiromi Nakamura [b], Takaji Wakita [a], Naokazu Takeda [a,3], Hironori Sato [b]

[a] Department of Virology II, National Institute of Infectious Diseases, Gakuen 4-7-1, Musashimurayama, Tokyo 208-0011, Japan
[b] Pathogen Genomics Center, National Institute of Infectious Diseases, Gakuen 4-7-1, Musashimurayama, Tokyo 208-0011, Japan
[c] Viral Diseases Research Team, National Institute of Animal Health, Tsukuba, Ibaraki 305-0856, Japan

ARTICLE INFO

Article history:
Received 6 June 2009
Returned to author for revision 7 July 2009
Accepted 7 August 2009
Available online 10 September 2009

Keywords:
Calicivirus
Substrate specificity
3C-like protease

ABSTRACT

To address the regulation and evolution of precursor protein cleavability in caliciviruses, we examined constraints on diversity of upstream regions of calicivirus precursor cleavage sites. We performed alanine scanning and supplementary mutagenesis of amino acids at P1, P2, P3, and P4 sites using four viruses representing the four major genera of the family *Caliciviridae*. This study complements previous mutagenesis studies and shows strong restrictions in mutations at the P1 and P4 sites for effective cleavage reactions. By contrast, such restrictions were less frequently observed at the P2 and P3 sites. Shannon entropy analysis of the reported sequences showed that the P2, P3, and P4 sites allow variations in amino acid size within a calicivirus genus whereas the P1 sites do not. Notably, the human sapovirus precursor protein exceptionally retains a basic rather than aromatic amino acid at the P4 site of the NS4/NS5 cleavage site in reported strains, and a substitution from basic to aromatic amino acid significantly enhanced cleavability at this site. Taken together, these data suggest the existence of (i) structural constraints on the P1 site that restrict size changes within each calicivirus genus, (ii) plastic substrate surfaces that accommodate size variation at the P2, P3, and P4 sites and modulate their own cleavabilities, and (iii) biological constraints on the P4 site that maintain the lower cleavability of the NS4/NS5 site in sapovirus.

© 2009 Elsevier Inc. All rights reserved.

Introduction

Caliciviruses are non-enveloped RNA viruses whose virus particles contain a single-stranded, positive-sense, polyadenylated RNA genome of about 7.3–8.3 kb with either two or three open reading frames (ORFs). Caliciviruses are currently classified into four major genera, *Sapovirus, Norovirus, Lagovirus*, and *Vesivirus*, on the basis of genome structure and diversity (Green, 2007). Relatively well-characterized representatives of these four genera are *Sapporo virus* (SaV), *Norwalk virus* (NoV), *Rabbit hemorrhagic disease virus* (RHDV), and *Feline calicivirus* (FCV), respectively.

The calicivirus RNA genome encodes a cysteine protease, termed a 3C-like protease, in ORF1 (Clarke and Lambden, 1997). The protease is initially synthesized as a part of ORF1 and cleaves the ORF1 polyprotein into multiple mature proteins (Clarke and Lambden, 2000). In the case of *Vesivirus*, viral protease additionally cleaves ORF2-encoded protein and generates the mature capsid protein VP1 (Matsuura et al., 2000; Oehmig et al., 2003; Rinehart-Kim et al., 1999; Sosnovtsev et al., 2002, 1998). The critical role of Cys in the calicivirus protease motif GDCG in the cleavage activity has been determined previously (Boniotti et al., 1994; Liu et al., 1996; Oka et al., 2005; Sosnovtseva et al., 1999). This processing is essential for generating infectious mature virus particles (Sosnovtsev et al., 2002, 1998).

The calicivirus protease cleaves peptide bonds downstream of the glutamic acid (E) or glutamine (Q) in the precursor protein (Green, 2007). However, these amino acid residues are found frequently in non-cleavage sites of viral precursor proteins, indicating that additional amino acids participate in recognition and cleavage by viral proteases. Consistently, previous mutagenesis studies have suggested that amino acids immediately upstream of the scissile bonds of the substrates play important roles in determining substrate cleavage specificity and efficiency (Belliot et al., 2003; Hardy et al., 2002; Robel

* Corresponding author. Department of Virology II, National Institute of Infectious Diseases, Gakuen 4-7-1, Musashimurayama, Tokyo 208-0011, Japan. Fax: +81 42 561 4729.
E-mail address: oka-t@nih.go.jp (T. Oka).
[1] These authors contributed equally to this study.
[2] Present address: Kitasato Research Center for Environmental Science, 1-15-1 Kitasato, Sagamihara-shi, Kanagawa 228-8555, Japan.
[3] Present address: Research Collaboration Center on Emerging and Re-emerging Infections, National Institute of Health, Department of Medical Sciences, Ministry of Public Health, Tivanond 14 Road, Muang, Nonthaburi 11000, Thailand.

0042-6822/$ – see front matter © 2009 Elsevier Inc. All rights reserved.
doi:10.1016/j.virol.2009.08.018

et al., 2008; Scheffler et al., 2007, 1998; Wirblich et al., 1995). These studies were exclusively done with a single virus strain at a time; in addition, they focused on particular P positions of cleavage sites. No studies have systemically analyzed the set of P1, P2, P3, and P4 positions of the cleavage site, numbered according to the method of Schechter and Berger (1967). Furthermore, a mutagenesis study at the P2 and P4 positions is lacking in *Vesivirus*.

To extend previous findings and obtain new information on the regulation and evolution of precursor protein cleavability in caliciviruses, we examined here constraints on the diversity of the regions upstream of calicivirus precursor cleavage sites. We conducted mutagenesis of amino acids at the P1, P2, P3, and P4 sites of representative cleavage sites of SaV, NoV, RHDV, and FCV precursors. A total of 34 mutants examined in this study have not been fully reported previously; therefore, our results complement those of previous mutagenesis studies. Furthermore, we also examined variations in size and chemical properties of the amino acids at the P1, P2, P3, and P4 positions within each calicivirus genus, using reported precursor sequences and Shannon entropy scores (Motomura et al., 2008; Naganawa et al., 2008; Shannon, 1997). Together with previous mutagenesis studies, our study provides a basis to understand both structural and biological constraints on the diversity of regions upstream of the proteolytic cleavage sites of the calicivirus precursor proteins.

Results

Site-directed mutagenesis of SaV P1, P2, P3, and P4 positions

The SaV strain Mc10, whose ORF1 polyprotein is 2278 aa in length and whose six cleavage sites have been experimentally determined (Oka et al., 2006), was used as the starting material for the present mutagenesis (Fig. 1A). A panel of ORF1 mutants having a single amino acid substitution at regions immediately upstream of cleavage sites was constructed with pUC19/SaV Mc10 full-length (see Materials and methods). A wild-type ORF1 (Pro^{w}) (Fig. 1B; lane Pro^{w}, filled arrowheads) and an ORF1 mutant having a C1171A mutation at the catalytic site of protease (Pro^{mut}) (Fig. 1B; lane Pro^{mut}, a open arrowhead) were included in the study as positive and negative controls for the ORF1 polyprotein processing, respectively (Oka et al., 2005, 2006, 2007). Alanine substitution mutants at the P1 position of the NS1/2, NS2/3, NS3/4, NS5/6-7, and NS6-7/VP1 cleavage sites (Fig. 1B; E69A, Q325A, Q666A, E1055A, and E1722A) and a double alanine mutant at the P2 and P1 positions of the NS4/5 cleavage site (Fig. 1B; E939A, E940A) were included in the study as controls to inhibit the individual cleavage sites (Oka et al., 2006).

When Pro^{w} was expressed and incubated for 3 h, more than 10 products were detected, among which 9 products corresponded in size to mature or relatively stable intermediate proteins, such as NS1, NS2, NTPase (NS3), 3A (NS4), VPg (NS5), NS2-3, 3A-VPg (NS4-5), 3A-VPg-ProPol (NS4-5-6-7), and VP1 (Fig. 1B; lane Pro^{w}, filled arrowheads). As reported previously (Oka et al., 2005, 2006), these products were not detected with the Pro^{mut} translation product; instead, a high-molecular-weight protein corresponding to the full-length ORF1 was detected (Fig. 1B; lane Pro^{mut}, a open arrowhead). The results indicate that the nine products in the Pro^{w} sample were the proteolytic products of the ORF1 precursor protein. Precise origin of the approximately 70-kDa product is difficult to elucidate because this band is visible when ORF1 polyprotein containing either wild or mutant protease was expressed (Fig. 1B; lanes Pro^{w} and Pro^{mut}) (Oka et al., 2005).

Aberrant processing patterns of the SaV mutant ORF1s as compared with those of the Pro^{w} ORF1 were frequently detected (Fig. 1B; F66A to E1722A, bold letters). For example, when an alanine substitution was introduced at the P4 or P1 position of the NS1/2 cleavage site, processing patterns were partially different from those of Pro^{w} (Fig. 1B; F66A and E69A); the amounts of mature NS1 and NS2 products decreased, the NS2-3 intermediate disappeared, and a novel band roughly corresponding to the size of the unprocessed NS1-2 intermediate appeared in the P4 and P1 site mutants (Fig. 1B; F66A and E69A, asterisks). The novel band of the F66A sample was somehow slightly larger than that of the E69A sample. However, both products specifically reacted with the anti-A antibody (Oka et al., 2005) by immunoprecipitation (data not shown), indicating that they are related to the unprocessed NS1-2 intermediate products. Together, the results suggest severe attenuation of NS1/2 cleavability by P4 or P1 single-site mutation. By contrast, no significant differences were detected with the P3- and P2-site mutants of the NS1/2 cleavage region as compared with Pro^{w} (Fig. 1B; T67A and E68A). From these results, we concluded that both the P4 and P1 residues are important for the processing at the NS1/2 cleavage site while the P3 and P2 residues are not necessarily critical to the substrate cleavability.

The crucial roles of the P4 site in the SaV ORF1 polyprotein processing were further evaluated with other five cleavage sites, NS2/3, NS3/4, NS4/5, NS5/6-7, and NS6-7/VP1, in the ORF1 polyprotein, because the amino acid residues at the P4 position of individual cleavage sites are highly conserved among the SaV strains (Oka et al., 2006). Similarly, effects of single mutations at the P1 site with the four cleavage sites and double mutation at P2 and P1 with the NS4/5 site were examined. Aberrant processing patterns were detected in four mutants with an alanine substitution at the P4 position (Fig. 1B; F322A, F663A, Y1052A, and F1719A) and four mutants with an alanine substitution at the P1 position (Fig. 1B; Q325A, Q666A, E1055A, and E1722A). The aberrant cleavage patterns of the ORF1 polyprotein in the P1 and the P4 mutants were very similar when the same cleavage sites were compared. Newly appeared (asterisks), decreased, or disappeared bands in the mutants could be explained by decreased efficiencies of cleavages around the mutation sites (Fig. 1B).

The P4 site in SaV is generally occupied by either an aromatic or hydrophobic amino acid (Fig. 1A) (Oka et al., 2006). However, the P4 site of the NS4/NS5 cleavage site exclusively has a basic amino acid in all human SaV strains reported thus far. An alanine substitution at the P4 position of the NS4/NS5 cleavage site did not cause significant processing defects (Fig. 1B; R937A), but a substitution from arginine (R) to F resulted in a drastic increase in amounts of mature NS4 and NS5 products (Fig. 1B; R937F). These increases were accompanied by the disappearance of NS4-5 and NS4-5-6-7 intermediate products, suggesting enhancement of the cleavability of the NS4-5 boundary by the R-to-F mutation. In contrast, a substitution from one aromatic to another aromatic amino acid substitution (Y to F) at the P4 position of the NS5/6-7 cleavage site did not cause significant processing defects or enhancement (Fig. 1B; Y1052F).

Together, our mutagenesis study has demonstrated that the aromatic amino acids (F or Y) at the P4 position of the NS1/NS2, NS2/NS3, NS3/NS4, NS5/NS6-7, and NS6-7/VP1 cleavage sites play a key role in maintaining relatively high levels of substrate cleavability and that R at the P4 position of NS4/NS5 plays a key role in suppressing cleavability at this site.

Site-directed mutagenesis of NoV P1, P2, P3, and P4 positions

The NoV strain U201, whose ORF1 polyprotein is 1702 aa in length (Katayama et al., 2006), was used as the starting material for the mutagenesis. Cleavage sites of the U201 ORF1 polyprotein were assigned on the basis of information on a processing map of other NoV strains (Belliot et al., 2003; Green, 2007) and sequence alignment (Fig. 2A). A wild-type ORF1 (Pro^{w}) and an ORF1 mutant having a C1150A mutation at the catalytic site of protease (Pro^{mut}) were

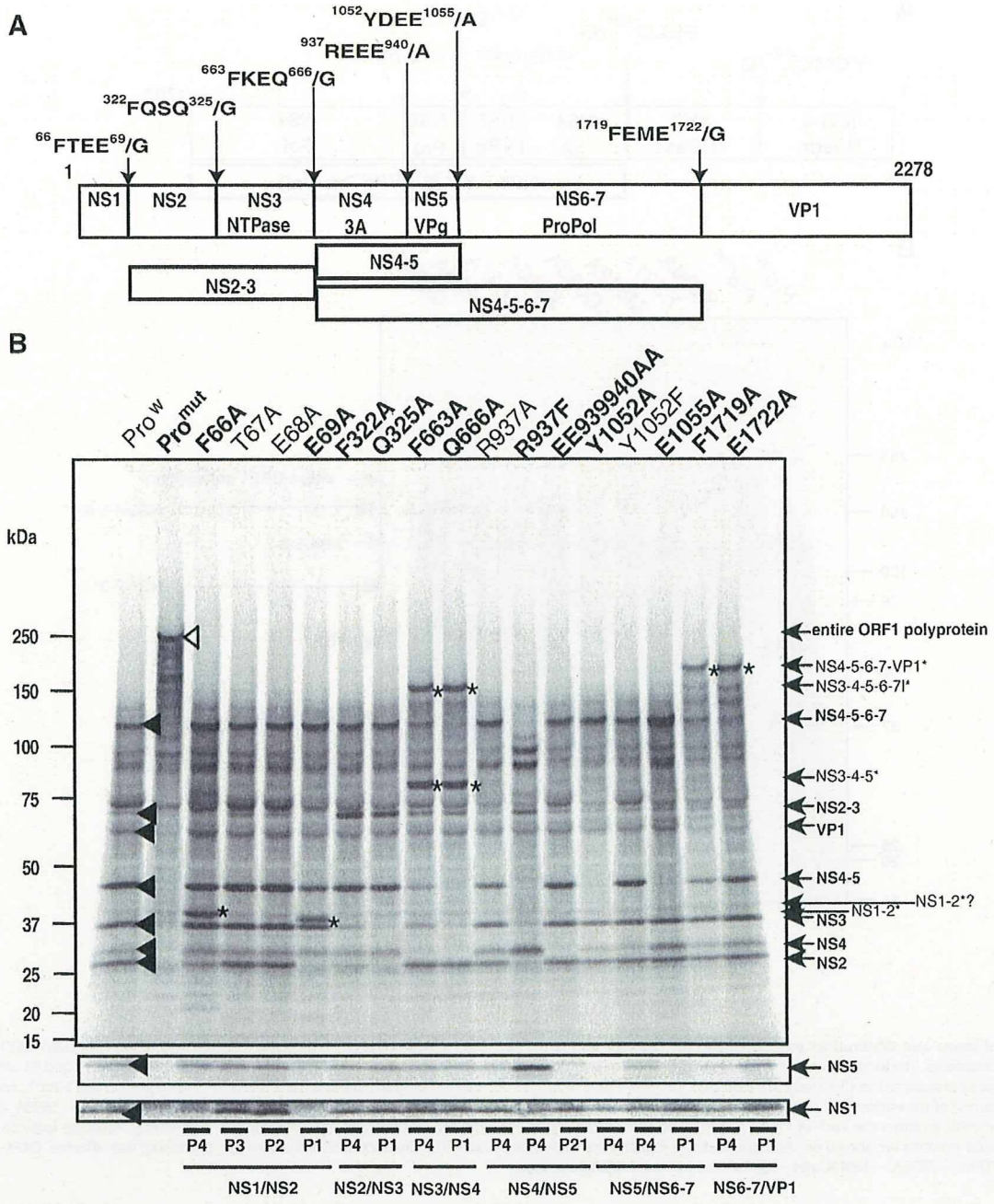

Fig. 1. Effects of amino acid substitutions introduced into the cleavage sites of the SaV ORF1 polyprotein. (A) Schematic representation of proteolytic cleavage sites of SaV Mc10 ORF1 polyprotein, P4, P3, P2, P1, and P1′ amino acid residues for the cleavage sites, and processing intermediates (Oka et al., 2006). (B) SDS-PAGE of *in vitro* ^{35}S-labeled proteins derived from the wild-type sequence, ORF1-Pro^{w}, and ORF1-Pro^{C1171A} (ORF1-Pro^{mut} forms) of the entire ORF1 region (aa 1–2278) and 16 mutants: ORF1-F66A, −T67A, −E68A, −E69A, −F322A, −Q325A, −F663A, −Q666A, −R937A, −R937F, −E939A, E940A, −Y1052A, −Y1052F, −E1055A, −F1719A, and −E1722A. NS1 and NS5 were immunoprecipitated with region-specific antibodies, anti-A and anti-D (Oka et al., 2005), respectively. The protein bands specific to either the Pro^{w} or Pro^{mut} forms of the entire ORF1 regions are indicated by filled and open arrowheads, respectively. Asterisks indicate newly appearing products. The viral proteins are shown on the right, and size markers are shown on the left. Thirteen mutants – ORF1-Pro^{mut}, −F66A, −E69A, −F322A, −Q325A, −F663A, −Q666A, −R937F, −E939A, E940A, −Y1052A, −E1055A, −F1719A, and −E1722A – in which the proteolytic processing was affected are indicated in boldface type.

included in the study as positive and negative controls for the ORF1 polyprotein processing, respectively.

When Pro^{w} was expressed and incubated for 3 h, several products corresponding in size to the Nterm (NS1-2), NTPase (NS3), Pol (NS7), and 3A-VPg-Pro-Pol (NS4-5-6-7) proteins were detected (Fig. 2B; Pro^{w}, filled arrowheads), as in another study (Belliot et al., 2003). Further incubation for up to 16 h resulted in the generation of additional products corresponding to the 3A (NS4), Pro (NS6), 3A-VPg (NS4-5), and Pro-Pol (NS6-7) proteins (data not shown). In contrast, when Pro^{mut} was expressed and incubated for 3 h, generation of these products was severely suppressed. Instead, a product corresponding to the entire ORF1 polyprotein was predominantly detected (Fig. 2B; Pro^{mut}, open arrowhead). These results showed that two of the cleavage sites, NS1-2/NS3 and NS3/NS4, were cleaved more efficiently than the others (Figs. 2A and B). Therefore, we examined the role of the four amino acid residues upstream of these two sites in the

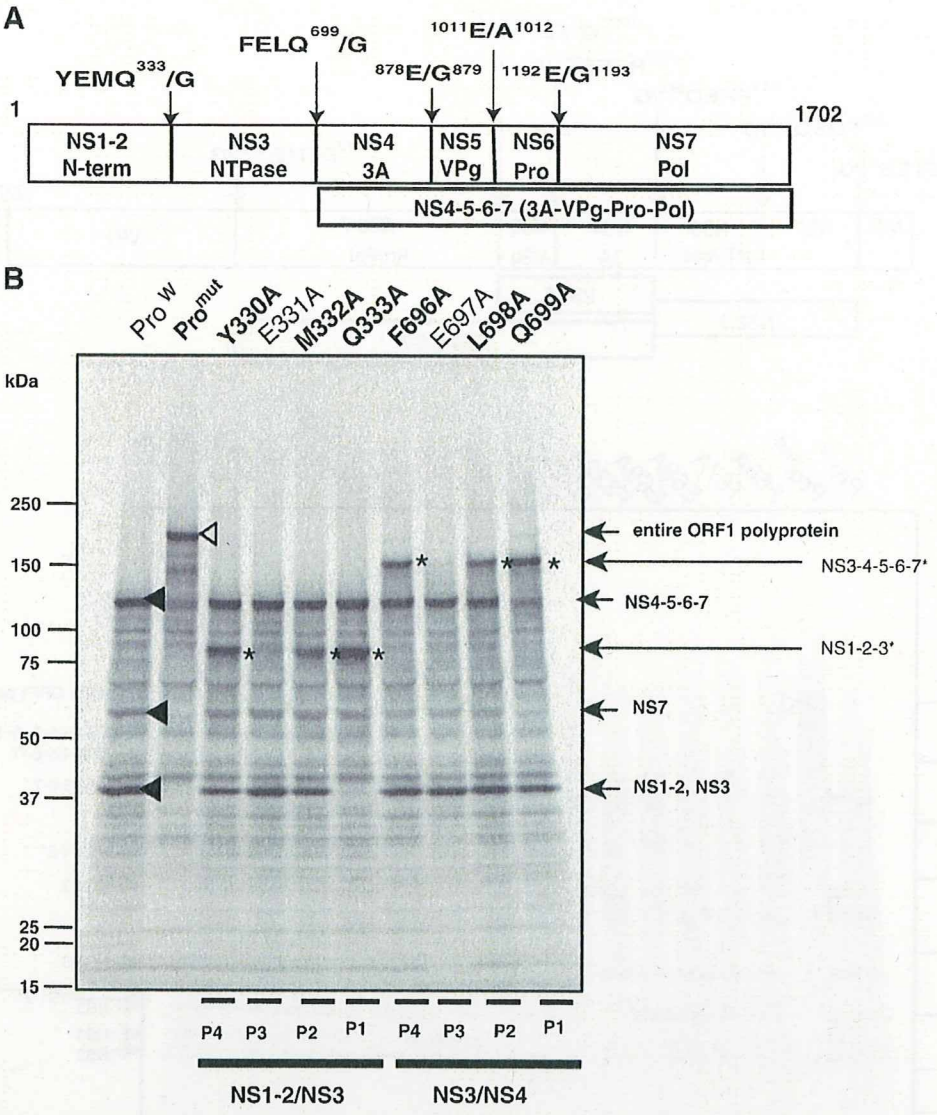

Fig. 2. Effects of amino acid substitutions introduced into the cleavage sites of the NoV ORF1 polyprotein. (A) Proteolytic cleavage map of the NoV U201 ORF1 polyprotein and processing intermediates. The locations and designations of the proteins have already been identified (Belliot et al., 2003; Green, 2007). The P4, P3, P2, P1 and P1′ amino acid residues for two cleavage sites analyzed in this study are indicated. (B) SDS–PAGE of *in vitro* ^{35}S-labeled proteins derived from the wild-type sequence, ORF1-Pro^{w}, and ORF1-Pro^{C1150A} (ORF1-Pro^{mut} forms) of the entire ORF1 region (aa 1–1702) as well as eight mutants: ORF1-Y330A, −E331A, −M332A, −Q333A, −F696A, −E697A, −L698A, and −Q699A. The protein bands specific to either the Pro^{w} or Pro^{mut} forms of the entire ORF1 region are indicated by filled and open arrowheads, respectively. Asterisks indicate newly appearing products. The viral proteins are shown on the right, and size markers are shown on the left. The mutants in which proteolytic processing was affected, ORF1-Pro^{mut}, −Y330A, −M332A, −Q333A, −F696A, −L698A, and −Q699A, are indicated in boldface type.

cleavability of the ORF1 polyprotein by mutating each residue to alanine in turn.

Aberrant processing patterns of the NoV mutants ORF1 as compared with those of the Pro^{w} ORF1 were frequently detected (Fig. 2B Y330A to Q699A, bold letters). When an alanine substitution was introduced at the P4, P2, or P1 position of the NS1-2/NS3 or the NS3/NS4 cleavage site, processing patterns that were partially different from those of Pro^{w} were detected; a novel band roughly corresponding in size to unprocessed intermediate products appeared with these mutants (Fig. 2B, asterisks). The appearance of these new products could be explained by attenuation of cleavability at the mutation sites. By contrast, no significant differences were detected in the P3 site mutants of the NS1-2/NS3 and NS3/NS4 cleavage regions as compared with Pro^{w} (Fig. 2B; E331A and E697A).

Together, our mutagenesis study has demonstrated that the amino acid residues at the P4, P2, and P1 positions of the NS1-2/NS3 and NS3/NS4 cleavage sites of NoV play key roles in determining efficient substrate cleavability.

Site-directed mutagenesis of RHDV P1, P2, P3, and P4 positions

The novel RHDV strain Hokkaido, with an ORF1 polyprotein 2344 aa in length (Fig. 3A), was used as the starting material for the present mutagenesis. Cleavage sites of the Hokkaido ORF1 polyprotein were assigned on the basis of information on the processing map of another RHDV strain (Meyers et al., 2000; Wirblich et al., 1995; Wirblich et al., 1996) and sequence alignment (Fig. 3A). The wild-type ORF1 (Pro^{w}) and an ORF1 mutant having a C1212A mutation at the catalytic site (Pro^{mut}) were included for the study as positive and negative controls for the ORF1 polyprotein processing, respectively. The NS3/NS4 site of the RHDV ORF1 polyprotein (Fig. 3A) was selected in the present study.

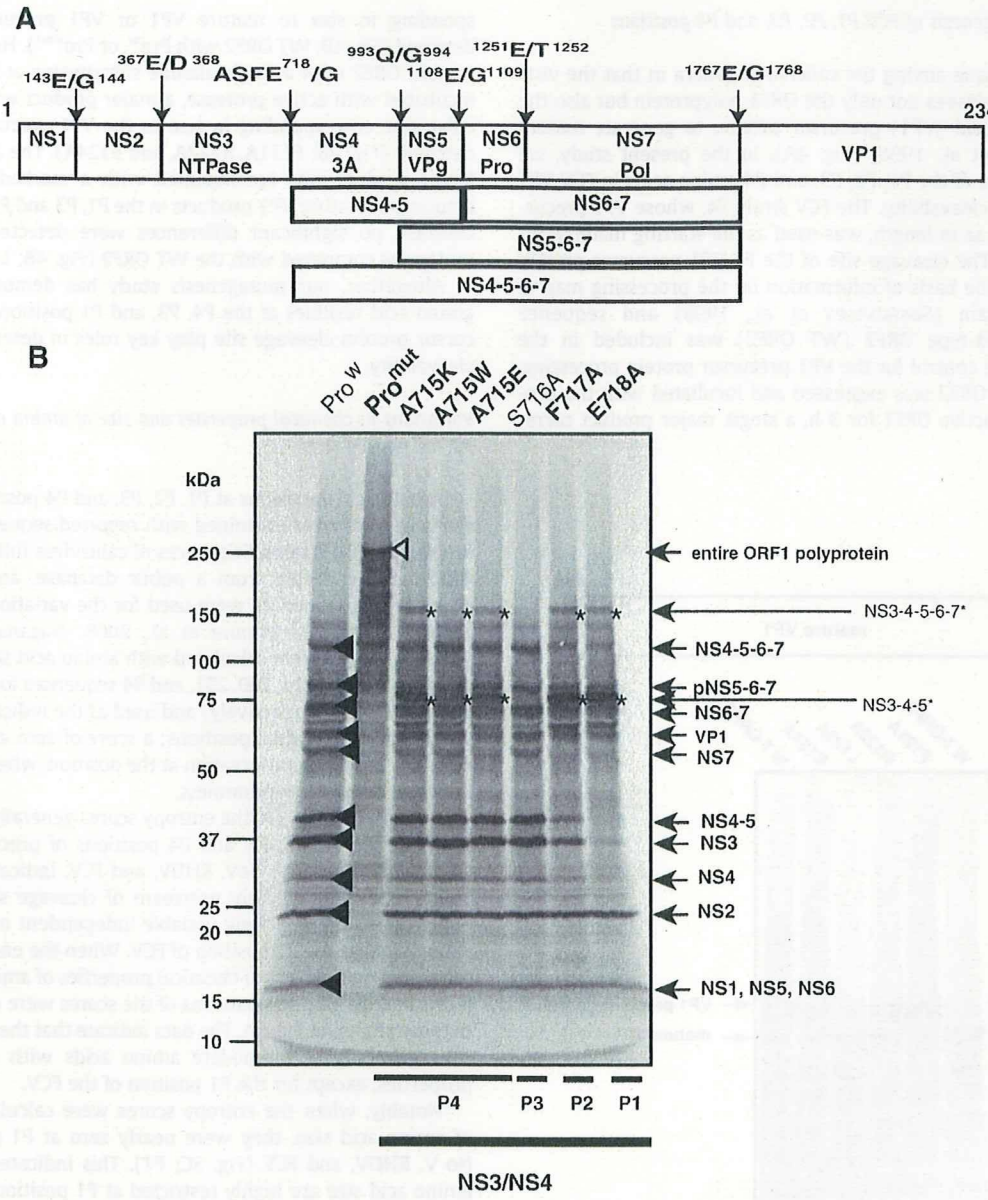

Fig. 3. Effects of amino acid substitutions introduced into the cleavage sites of the RHDV ORF1 polyprotein. (A) Proteolytic cleavage map of the RHDV Hokkaido ORF1 polyprotein and processing intermediates. The locations and designations of the proteins have been adopted (Martin Alonso et al., 1996; Meyers et al., 2000; Wirblich et al., 1996). The P4, P3, P2, P1, and P1′ amino acid residues of the cleavage site in the ORF1 polyprotein analyzed in this study are indicated. (B) SDS–PAGE of *in vitro* ^{35}S-labeled proteins derived from the wild-type sequence, ORF1-Pro^{w}, and ORF1-Pro^{mut} forms of the entire ORF1 region (aa 1–2344) as well as six mutants: ORF1-A715K, −A715W, −A715K, −S716A, −F717A, and −E718A. The protein bands specific to either ORF1-Pro^{w} or ORF1-Pro^{C1212A} (ORF1-Pro^{mut} forms) of the entire ORF1 region are indicated by filled and open arrowheads, respectively. Asterisks indicate newly appearing products. The viral proteins are shown on the right, and size markers are shown on the left. Six mutants in which proteolytic processing was affected – ORF1-Pro^{mut}, −A715K, −A715W, −A715K, −F717A, and −E718A – are indicated in boldface type.

When Pro^{w} was expressed and incubated for 3 h, products corresponding in size to the NS1, NS2, NTPase (NS3), 3A (NS4), VPg (NS5), Pro (NS6), Pol (NS7), 3A-VPg (NS4-5), Pro-Pol (NS6-7), VPg-Pro-Pol (NS5-6-7), 3A-VPg-Pro-Pol (NS4-5-6-7), and VP1 proteins were detected (Fig. 3B; Pro^{w}, filled arrowheads). In contrast, when Pro^{mut} was expressed and incubated for 3 h, the generation of these products was severely suppressed, and instead a product corresponding to the entire ORF1 polyprotein was predominantly detected (Fig. 3B; Pro^{mut}, open arrowheads).

Aberrant processing patterns of the RHDV mutants ORF1 as compared with those of the Pro^{w} ORF1 were frequently detected (Fig. 3B A715K to E718A, bold letters). An alanine substitution was introduced at the P3, P2, or P1 position of the NS3/NS4 cleavage site, and other substitution was introduced at the P4 position at this site because the native aa for residue 715 at P4 position is A (Fig. 3A). The processing patterns that were partially different from those of Pro^{w} were detected: novel bands roughly corresponding to the size of unprocessed intermediate products appeared with these mutants (Fig. 3B, asterisks). The appearance of these new products could be explained by the attenuation of cleavability at the NS3/NS4 site.

By contrast, no significant differences were detected between the P3 site mutant and Pro^{w} (Fig. 3B; S716A). Together, our mutagenesis study has demonstrated that the amino acid residues at P4, P2, and P1 of the NS3/NS4 cleavage site of RHDV play key roles in determining substrate cleavability.

Site-directed mutagenesis of FCV P1, P2, P3, and P4 positions

Vesivirus is unique among the calicivirus genera in that the viral protease in ORF1 cleaves not only the ORF1 polyprotein but also the ORF2-encoded capsid (VP1) precursor protein to generate mature VP1 (Sosnovtsev et al., 1998) (Fig. 4A). In the present study, we examined the roles of the P1, P2, P3, and P4 amino acids in FCV VP1 precursor protein cleavability. The FCV strain F4, whose VP1 precursor protein is 668 aa in length, was used as the starting material for the mutagenesis. The cleavage site of the F4 VP1 precursor protein was assigned on the basis of information on the processing map of another FCV strain (Sosnovtsev et al., 1998) and sequence alignment. A wild-type ORF2 (WT ORF2) was included in the study as a positive control for the VP1 precursor protein processing.

When the WT ORF2 was expressed and incubated with the protease active or inactive ORF1 for 3 h, a single major product corresponding in size to mature VP1 or VP1 precursor protein was detected (Fig. 4B; WT ORF2 with Pro^{w}, or Pro^{mut}). However, when the mutant ORF2 with a single alanine substitution at P4, P3, or P1 was incubated with active protease, a major product with a larger molecular size, corresponding in size to the VP1 precursor protein, was detected (Fig. 4B; F121A, R122A, and E124A). The appearance of the larger product was accompanied with a marked decrease in the amounts of mature VP1 products in the P1, P3 and P4 site mutants. By contrast, no significant differences were detected in the P2 site mutant as compared with the WT ORF2 (Fig. 4B; L123A).

Altogether, our mutagenesis study has demonstrated that the amino acid residues at the P4, P3, and P1 positions of the VP1 precursor protein cleavage site play key roles in determining substrate cleavability.

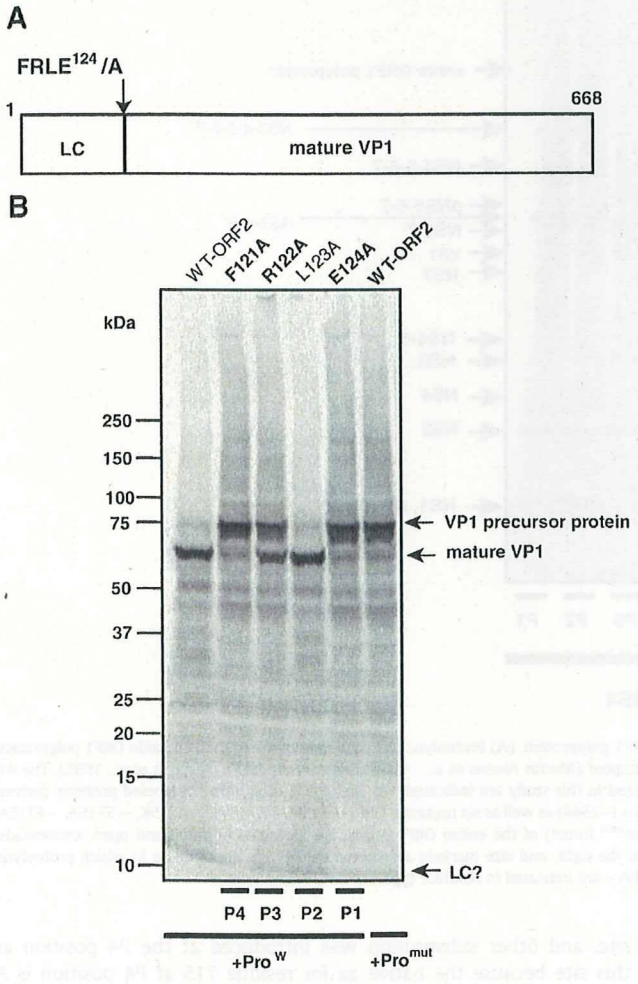

Fig. 4. Effects of amino acid substitutions introduced into the cleavage site of the FCV capsid precursor protein. (A) Cleavage map of the FCV F4 capsid (VP1) precursor protein. The P4, P3, P2, P1, and P1′ amino acid residues at the cleavage site in the capsid precursor protein have been adopted from Sosnovtsev et al. (1998). (B) SDS–PAGE of *in vitro* ^{35}S-labeled proteins derived from the wild-type sequence, ORF2-native, of the entire ORF2-encoded protein (aa 1–668), and four mutants (ORF2-F121A, −R122A, −L123A, and −E124A) that were incubated with non-radiolabeled FCV F4 ORF1 polyprotein as a source of protease in trans. ORF2 native was also incubated with non-radiolabeled FCV F4 ORF1 polyprotein with protease mutant in trans. The viral proteins are shown on the right, and size markers are shown on the left. The three mutants – ORF2-F121A, −R122A, and −E124A – with active protease and the ORF2 native with inactive protease showing affected proteolytic processing are indicated in boldface type.

Variations in chemical properties and size of amino acids at the P1, P2, P3, and P4 sites

Amino acid variations at P1, P2, P3, and P4 positions of precursor cleavage sites were examined with reported sequences of SaV, NoV, RHDV, and FCV strains. Sequences of calicivirus full-length ORF1 and ORF2 were collected from a public database, and a total of 589 cleavage site sequences were used for the variation study. Shannon entropy scores (Motomura et al., 2008; Naganawa et al., 2008; Shannon, 1997) were calculated with amino acid sequences for each virus group ($n = 114$, 160, 231, and 84 sequences for SaV, NoV, RHDV, and FCV strains, respectively) and used as the indicator of amino acid variations at individual positions; a score of zero at a given position indicates absolute conservation at the position, whereas a score of 4.4 indicates complete randomness.

As shown in Fig. 5A, the entropy scores generally ranged from 1.0 to 3.0 at the P1, P2, P3, and P4 positions of precursor polyprotein cleavage sites of SaV, NoV, RHDV, and FCV, indicating that the four amino acids immediately upstream of cleavage sites of calicivirus polyproteins are relatively variable independent of viral genera. An exception was the P1 position of FCV. When the entropy scores were calculated on the basis of chemical properties of amino acids (Fig. 5B), levels and distribution patterns of the scores were essentially similar to those shown in Fig. 5A. The data indicate that the P1, P2, P3, and P4 sites generally accommodate amino acids with distinct chemical properties, except for the P1 position of the FCV.

Notably, when the entropy scores were calculated on the basis of amino acid size, they were nearly zero at P1 positions for SaV, No V, RHDV, and FCV (Fig. 5C; P1). This indicates that changes in amino acid size are highly restricted at P1 positions independent of viral genera. In contrast, the entropy scores are around 1.0 at the P2, P3, and P4 positions for SaV, NoV, RHDV, and FCV (Fig. 5C; P2, P3, and P4). These data indicate that calicivirus P2, P3, and P4 sites allow greater variations in amino acid size than the P1 site.

Discussion

Previous mutagenesis studies have reported important roles of amino acids immediately upstream of the calicivirus cleavage sites using different cleavage sites, different virus strains, and different assessment systems of cleavage from ours (Belliot et al., 2003; Robel et al., 2008; Scheffler et al., 2007; Sosnovtsev et al., 1998; Wirblich et al., 1995) (Supplemental Table 1). The present study extends their findings and provides new information regarding structural and biological constraints on calicivirus substrate diversity.

Present and previous mutagenesis studies have shown that amino acid substitutions at the P1 site mostly reduced cleavability of the junction of precursors. These mutations alter the size of side chains of P1 amino acids (Supplemental Table 1), suggesting a restriction against size changes in the P1 amino acids. Consistently, Shannon entropy analysis clearly showed that the P1 site does not

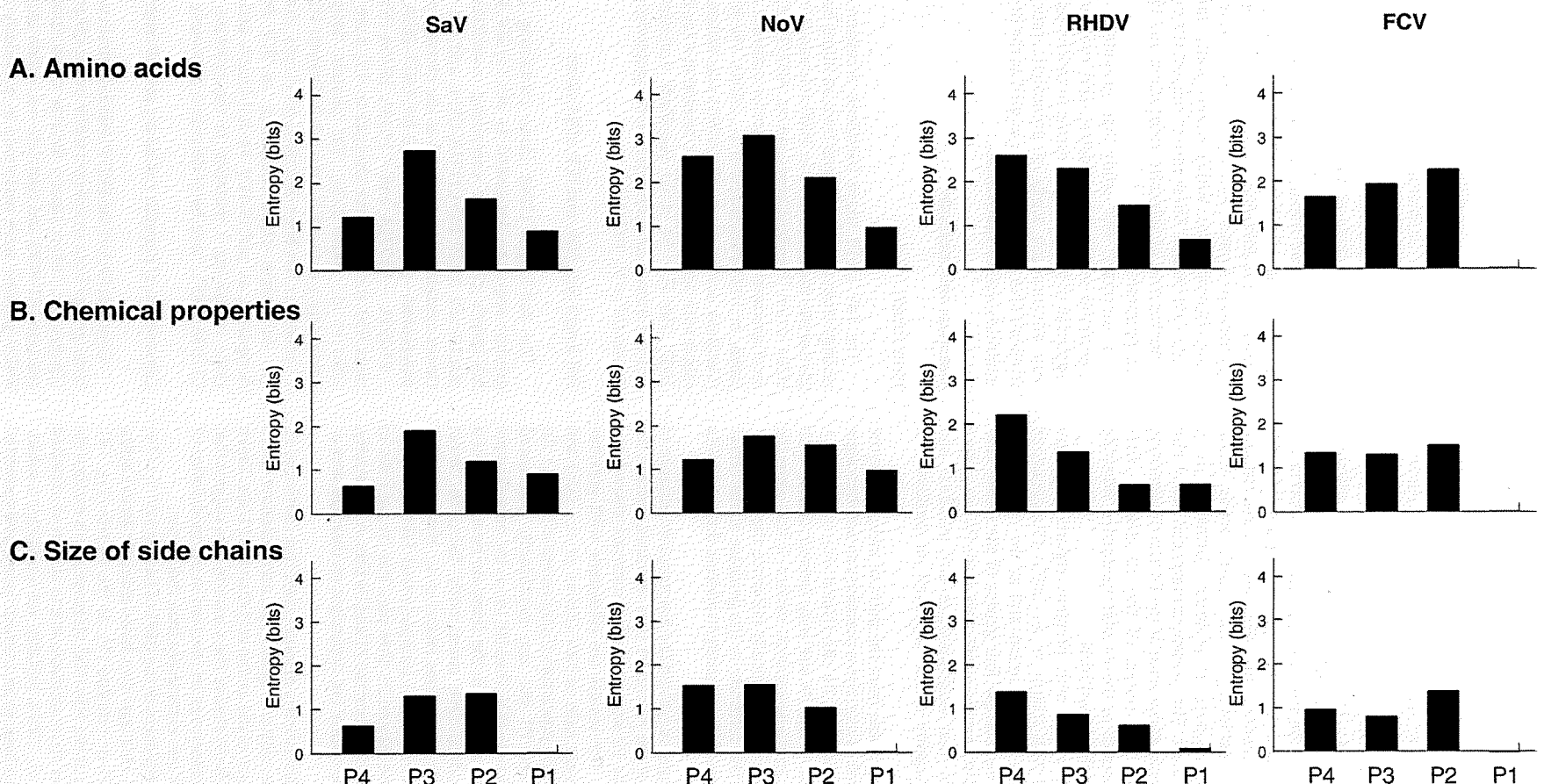

Fig. 5. Amino acid variations at P1, P2, P3, and P4 positions of calicivirus precursor cleavage sites. Shannon entropy scores representing variations at individual amino acid positions (Motomura et al., 2008; Naganawa et al., 2008; Shannon, 1997) were calculated using SaV ORF1, NoV ORF1, RHDV ORF1, and FCV ORF1/ORF2 sequences. A total of 589 cleavage site sequences were used ($n = 114$, 160, 231, and 84 amino acid sequences for SaV, NoV, RHDV, and FCV strains, respectively). The distribution of entropy scores in each viral genus is shown along with amino acid positions. An entropy score of zero indicates absolute conservation, whereas that of 4.4 indicates complete randomness. Entropy scores based on amino acids (A), chemical properties of amino acids (B), and size of side chains (C) are indicated.

allow variations in amino acid size within the genus of the family *Caliciviridae*. Taken together, these findings strongly suggest structural constraints on the P1 site that restrict size changes within each calicivirus genus (Belliot et al., 2003; Blakeney et al., 2003; Hardy et al., 2002; Liu et al., 1996; Meyers et al., 2000; Oka et al., 2006; Robel et al., 2008; Seah et al., 1999, 2003; Sosnovtsev et al., 2006, 2002, 1998; Wirblich et al., 1995).

This conclusion is also conceivable from the point of view of enzyme structure and reaction. The side chain of the P1 residue is located near the scissile bonds of the substrate (Nakamura et al., 2005). Therefore, changes in the size of side chains by mutation will critically influence conformation or steric positioning of the scissile bond in the protease active center. This could result in less efficient hydrolysis via improper positioning of the scissile bonds, water molecules, and catalytic residues of protease. Further study is necessary to clarify this issue. The present mutagenesis study also demonstrated the functional importance of the P4 site in regulating substrate cleavability in caliciviruses. Of the 10 cleavage sites examined, all single mutations at the P4 sites modulated substrate cleavability either negatively or positively.

The results were consistent with previous reports with SaV (Robel et al., 2008) and NoV (Hardy et al., 2002) (Supplemental Table 1). Interestingly, the size of amino acid at the P4 site was shown to be variable in each of the four genera of the family *Caliciviridae*. These data suggest that the amino acid at the P4 site plays a role as a key modulator that accommodates size variation and regulates substrate cleavability either negatively or positively in caliciviruses.

This conclusion is conceivable from the point of view of enzyme structure. The catalytic cleft of calicivirus protease can accommodate several amino acids including the P4 site (Nakamura et al., 2005). Therefore, the amino acid at the P4 site may interact closely with some amino acids of the protease catalytic surface. If this were the case, levels of interactions would critically influence the conformation or steric position of the substrate in the protease active center and thus the substrate cleavability. A study to address this possibility is now in progress.

While this study strongly suggested the functional importance of the P1 and P4 sites, that of the P2 and P3 sites remained unclear. An alanine substitution at the P2 site attenuated substrate cleavability only in NoV and RHDV. The results are consistent with previous reports on different cleavage sites of NoV (Belliot et al., 2003) and RHDV (Wirblich et al., 1995) precursors (Supplemental Table 1). An alanine substitution at the P3 site also significantly attenuated substrate cleavability only with FCV. Thus far, this is the only example of positive involvement of a P3 site in the substrate cleavability of a calicivirus; previous studies have consistently failed to detect influences on cleavage by P3 mutations (Robel et al., 2008; Scheffler et al., 2007; Sosnovtsev et al., 2002) (Supplemental Table 1). These results may imply that the P2 and P3 sites play less crucial roles in substrate cleavage in calicivirus than the P1 and P4 sites. Alternatively, the roles they play may be critical but dependent on cleavage sites or viral genera.

Shannon entropy analysis clearly demonstrated that calicivirus P2 and P3 sites are variable within a genus and accommodate much greater variations in the size of the amino acid than the P1 site. Taken together with the mutagenesis results, the variation data suggest that the P2 and P3 sites may sometimes be involved in the modulation of substrate cleavability, but less extensively than the P4 site.

Reported full-length sequences of the ORF1 of human SaV ($n = 19$) show that five of the six cleavage sites have aromatic amino acids, such as phenylalanine (F) or tyrosine (Y), at the P4 site (Fig. 1A). However, the P4 position of the NS4/NS5 cleavage site is exclusively occupied by a basic rather than aromatic amino acid in all reported strains (Fig. 1A) (Oka et al., 2006). Notably, we found that a substitution at this P4 site from a basic to an aromatic amino acid converted the cleavage site phenotype from low to high sensitivity to sapovirus protease. These findings suggest the existence of biological constraints on the P4 site to maintain a lower cleavability of the NS4/NS5 site in sapovirus. Such differential cleavability among cleavage sites of a precursor is reported to be essential for producing mature infectious viruses in other positively stranded RNA viruses (Gorchakov et al., 2008; Pathak et al., 2008; Pettit et al., 1994; Wiegers et al., 1998). It would be interesting to evaluate whether the preservation of lower levels of cleavability at the NS4/NS5 cleavage site is required for effective virus replication in the sapovirus.

The functional importance of the P4 and P1 sites for substrate cleavability has also been reported in other positive-stranded RNA viruses, such as poliovirus (Blair and Semler, 1991; Pallai et al., 1989) and hepatitis A virus (Jewell et al., 1992). These viruses belong to the family *Picornaviridae*, which is genetically distantly related to the family *Caliciviridae*. These results suggest the evolutionary similarity in mechanisms of substrate recognition and cleavage among these viral proteases.

In summary, our study has provided some new bases to understand structural, biological, and evolutionary aspects of the regulation of precursor processing in caliciviruses. The obtained data may advance the study of proteolytic processing of positively stranded RNA virus precursors as well as the development of specific inhibitors against caliciviruses.

Materials and methods

Virus strains

The SaV Mc10 strain (GenBank accession no. AY237420) was isolated from a fecal specimen from an infant hospitalized with acute gastroenteritis in Thailand in 2000 (Hansman et al., 2004). The NoV U201 strain (GenBank accession no. AB039782) was isolated from a fecal specimen from a gastroenteritis outbreak at a hotel in Saitama, Japan, in 1998 (Kageyama et al., 2004). The RHDV Hokkaido strain (GenBank accession no. AB300693) was isolated from the liver of a rabbit with acute hemorrhagic disease in a zoo in Hokkaido, Japan, in 2002. The FCV F4 strain (GenBank accession no. D31836) was isolated from a cat with respiratory symptoms (Makino et al., 2006; Takahashi et al., 1971).

Full-length SaV, NoV, and FCV cDNA clones

The full-length cDNA clone containing a native SaV Mc10 genome sequence designated as pUC19/SaV Mc10 full-length, the full-length cDNA clone containing a mutation in the protease, pUC19/SaV Mc10 full-C1171A/ORF1, and the six full-length cDNA clones containing mutation(s) at the cleavage sites of the SaV ORF1 polyprotein—pUC19/SaV Mc10 full-ORF1-E69A, −Q325A, −Q666A, −E1055A, −E1722A, and −E939A, E940A (E's at amino acid positions 939 and 940 were changed to A's) have previously described (Oka et al., 2005, 2006). The plasmid designated as pT7U201F containing a native full-length NoV Saitama U201 genome with the T7 promoter has been described previously (Katayama et al., 2006). The full-length clone containing an FCV F4 genome sequence designated as pUC19/FCV F4 full-length and a full-length cDNA clone containing a mutation in the protease, pUC19/FCV F4 full-C1193A/ORF1, have been described previously (Oka et al., 2007).

Construction of plasmids containing the full-length RHDV genome

Genomic RNA of the RHDV Hokkaido strain was purified from liver homogenate from an infected rabbit by the QIAamp Viral RNA Mini Kit (Qiagen KK, Tokyo, Japan). Reverse transcription polymerase chain reaction (RT-PCR) and complete nucleotide sequence analysis of the RHDV genome were performed as previously described (Katayama

et al., 2002). A plasmid harboring the entire RHDV genome was constructed as follows: The 5′ fragment corresponding to nt 1-4832 was amplified with a sense primer (5′-CAGGGGCCCGGTACCCTGG**TA-ATACGACTCACTATA**GTGAAAGTTATGGCGGTTATGTCG-3′), which included a *Kpn*I site (underlined), a T7 RNA polymerase promoter sequence (bold), and an antisense primer (5′-CATCGGAGTCATGGCA-TAC-3′). The 3′ fragment corresponding to nt 3701-7413 was amplified with a sense primer (5′-GCTAGGGTTCTCAAAGATG-3′) and an antisense primer (5′-GAGGTGGAGATGCC ATGCCGACCCt_{30} ATAGCT-TACTTTAAAC-3′). HDV ribozyme and T7 terminator sequences were amplified from the pT7HCV09Luc plasmid (Yap et al., 1998) with a sense primer (5′-GGGTCGGCATGGCATCTCCACCTC-3′) and an antisense primer (5′-GAACTAGTGCGGCCGCGAGCTCAGATCTCCTTTCAG-CAAAAAACCCCTCAAG-3′), which included a *Not*I site (underlined). These three DNA fragments were purified from gel using the QIAquick Gel Extraction Kit (Qiagen). HDV ribozyme and T7 terminator sequences were joined with the 3′ fragment corresponding to nt 3701-7413 of the RHDV genome by primerless PCR as previously described (Katayama et al., 2006; Oka et al., 2007).

The amplified DNA fragment, designated as RHDV Hokkaido 3701-7413 polyA-Rz-T7 term, was purified and digested with *Mlu*I (unique site in the RHDV genome sequence) and *Not*I. To clone the RHDV genome sequence, *Xho*I, *Mlu*I, *Bgl*II, and *Not*I sites were added between the *Kpn*I and *Bam*HI sites in the pUC19 vector (Toyobo, Osaka, Japan). Then, the insert (RHDV Hokkaido 3701-7413 polyA-Rz-T7 term) was cloned into a modified pUC19 vector, which had been previously digested with *Mlu*I and *Not*I. The resultant plasmid was designated as RHDV Hokkaido 3′-polyA-Rz-T7 term/pUC19. Finally, the RHDV Hokkaido 5′ region corresponding to nt 1-4832 was digested with *Kpn*I and *Mlu*I (New England Biolabs) and then cloned into *Kpn*I- and *Mlu*I-digested RHDV Hokkaido 3′-polyA-Rz-T7 term/pUC19. The resultant plasmid containing a full-length RHDV Hokkaido genome sequence with the T7 promoter at the 5′ end, and the poly(A) tract, ribozyme, and T7 terminator at the 3′ end was designated as RHDV Hokkaido T7-GG full-length Rz-T7 term/pUC19 ver3 (pUC19/RHDV Hokkaido full-length). For plasmid cloning, *Escherichia coli* DH5α was used. The complete nucleotide sequence of the insert was determined to confirm the original sequence of the RHDV Hokkaido strain (GenBank accession number AB300693).

Site-directed mutagenesis

Site-directed mutagenesis was performed using the GeneTailor Site-Directed Mutagenesis System (Invitrogen), with pUC19/SaV Mc10 full-length (Oka et al., 2005), pT7U201F (Katayama et al., 2006), pUC19/RHDV Hokkaido full-length, and pUC19/FCV F4 full-length (Oka et al., 2007) as the templates. The site-directed mutagenesis primers in the protease-coding region and in the upstream of cleavage sites are listed in Table 1.

Ten SaV Mc10 full-length mutant cDNA clones containing a mutation in the upstream of cleavage sites – pUC19/SaV Mc10 full – F66A/ORF1, – T67A/ORF1, – E68A/ORF1, – F322A/ORF1, – F663A/ORF1, – R937A/ORF1, – R937F/ORF1, – Y1052A/ORF1, – Y1052F/ORF1, and – F1719A/ORF1 – were constructed. Nine NoV U201 full-length mutant cDNA clones containing a mutation in the protease or upstream of the cleavage sites – pT7 U201 full C1150A /ORF1, Y330A/ORF1, – E331A/ORF1, – M332A/ORF1, – Q333A/ORF1, – F696A/ORF1, – E697A/ORF1, – L698A/ORF1, and – Q699A/ORF1 – were constructed. Seven RHDV Hokkaido full-length mutant cDNA clones containing a mutation in the protease or upstream of the cleavage site – pUC19/RHDV Hokkaido full – C1212A/ORF1, – A715K/ORF1, – A715W/ORF1, – A715E/ORF1, – S716A/ORF1, – F717A/ORF1, and – E718A/ORF1 – were constructed. Four FCV F4 full-length mutant cDNA clones containing a mutation upstream of the cleavage site – pUC19/FCV F4 full – F121A/ORF2, – R122A/ORF2, – L123A/ORF2, and – E124A/ORF2 – were constructed. Clones were screened by sequence analysis, and plasmids containing the desired mutations in the protease or upstream of the cleavage sites were used to complete the genome sequence analysis. All of these full-length clones were verified by sequencing analysis to confirm the absence of additional mutations leading to amino acid changes.

In vitro-coupled transcription–translation assay

In vitro T7 polymerase-coupled transcription–translation in rabbit reticulocytes was performed using the TNT T7 Quick for PCR DNA kit (Promega, Madison, WI). The primers used to generate linear DNA fragments containing the T7 promoter are shown in Table 2. PCR was performed with 100 ng of full-length native or mutant cDNA clones as previously described (Oka et al., 2005, 2006, 2007). To express radiolabeled polyproteins, 3 μl of the PCR mixture was mixed with 20 μl of TNT T7 PCR Quick Master Mix (Promega) and 2 μl of Redivue Pro-mix L-[^{35}S] *in vitro* cell-labeling mix (GE Healthcare Biosciences), and the mixture was incubated at 30 °C for 3 or 16 h. The rate of cleavage for some mutants might be slower than the wild type but still go to completion in the 3 h incubations. After incubation, 4 μl of the reaction mixture was mixed with 20 μl of SDS–PAGE sample buffer (62.5 mM Tris–HCl (pH 6.8), 5% (w/v) sucrose, 2% (w/v) SDS, and 0.002% (w/v) bromophenol blue with 5% (v/v) 2-mercaptoethanol) and heated at 95 °C for 5 min; then 10 μl of the mixture was loaded onto 5% to 20% Tris–Gly polyacrylamide gel (D.R.C., Tokyo).

To express the non-radiolabeled polyproteins, 5 μl of the PCR mixture was mixed with 40 μl of TNT T7 PCR Quick Master Mix

Table 1
Oligonucleotides used for site-directed mutagenesis in the protease or in the upstream of the cleavage sites.

Mutant name[a]	Nucleotide sequence (5′–3′)[b]
SaV Mc10	
F66A	GCTGCCGCCCCCACAgccACGGAGGAGGGCTTG
T67A	GCCGCCCCCACATTCgcgGAGGAGGGCTTGTTAGACTC
E68A	GCCGCCCCCACATTCACGgcgGAGGGCTTGTTAGACTC
F322A	CTTGTTAAGAGCACGgccCAGTCACAAGGCCCAAC
F663A	CTTGATGGAAACCAAGgccAAGGAGCAGGGCAATGAAC
R937A	GCCACCCGGTCTGGTgcgGAGGAGGAGGCCAAAGG
R937F	GCCACCCGGTCTGGTtttGAGGAGGAGGCCAAAGGAAAG
Y1052A	CCCGTAATCAAGGTgccGATGAAGAAGCTCCCACACC
Y1052F	CCCGTAATCAAGGTtttGATGAAGAAGCTCCCACACC
F1719A	ACCACCAAATTAGTGgccGAAATGGAGGGCCTAGGC
NoV U201	
C1150A	ACAACACCAGGTGACgccGGGTGCCCCTACGTGTACAAG
Y330A	GCCCCCTTACTCGGTGACgccGAGATGCAGGGCCCAGAAG
E331A	GCCCCCTTACTCGGTGACTACgcgATGCAGGGCCCAGAAG
M332A	GCCCCCTTACTCGGTGACTACGAGgcgCAGGGCCCAGAAGAC
Q333A	GGTGACTACGAGATGgcgGGCCCAGAAGACCTG
F696A	CACGAGAGAATGGATGAGgccGAGCTCCAAGGCCCTAATCTAC
E697A	CGAGAGAATGGATGAGTTCgcgCTCCAAGGCCCTAATCTACC
L698A	GAGAATGGATGAGTTCGAGgccCAAGGCCCTAATCTACCAACC
Q699A	GAGAATGGATGAGTTCGAGCTCgcaGGCCCTAATCTACCAACC
RHDV Hokkaido	
C1212A	CAGACCACCCACGGGGACgcgGGGCTACCATTGTATG
A715K	AGTGAGCATCCTGATGTGaagTCGTTCGAAGGCGCTAAC
A715W	AGTGAGCATCCTGATGTGtggTCGTTCGAAGGCGCTAAC
A715E	AGTGAGCATCCTGATGTGgaaTCGTTCGAAGGCGCTAAC
S716A	ATCCTGATGTGGCCgcgTTCGAAGGCGCTAACAAATTC
F717A	ATCCTGATGTGGCCTCGgccGAAGGCGCTAACAAATTC
E718A	CCTGATGTGGCCTCGTTCgcaGGCGCTAACAAATTCAAC
FCV F4	
F121A	CCAAACCTACCGCTCgcccCGATTGGAGGCCGATG
R122A	CAAACCTACCGCTCTTCgcaTTGGAGGCCGATGATG
L123A	CCTACCGCTCTTCCGAgcgGAGGCCGATGATGGATC
E124A	CCGCTCTTCCGATTGgcgGCCGATGATGGATCC

[a] The name of the mutant represents the amino acid change. Amino acid is shown in the one-letter code. The letter before the number indicates the original amino acid residue, and the letter after the number indicates the mutant.

[b] Only the positive-sense oligonucleotide sequence is shown. The codon corresponding to changed amino acid is shown in lower case.

Table 2
PCR primers to prepare templates for in vitro transcription–translation.

Fragment[a]	Sequence (5′-3′)	Nucleotide positions	Amino acid positions
SaV entire ORF1	GCTTCCAAGCCATTCTACCCAATAGAG[b] TTCTAAGAACCTAACGGCCCGGc	17-6847	1-2278
NoV entire ORF1	AAGATGGCGTCTAACGACGCTTCCGTTG[b] TTCGACGCCATCTTCATTCACAAAACTG[c]	8-5110	1-1702
RHDV entire ORF1	GCGGTTATGTCGCGC[b] GACATAAGAAAAGCCATTAGTTGC[c]	13-7041	1-2344
FCV entire ORF1	TCTCAAACTCTGAGCTTCGTG[b] TCAAACTTCGAACACATCACAGTG[c]	23-5311	1-1763
FCV capsid precursor	TGCTCAACCTGCGCTAACGTG[b] TAATTTAGTCATTCTGCTCCTAATG[c]	5317-7317	1-668

[a] The AUG codon was derived from the original sequence.
[b] Upper line indicates forward primer, which includes 5′-GGATCC*TAATACGACTCACTATA*GGGAACAGCCACA**TG** containing the T7 promoter (underlined) and an additional start codon (bold) at the 5′ end.
[c] Lower line indicates reverse primer, which includes 5′-T30**TTA**-3′, corresponding to polyA with a stop codon (bold) at the 5′ end.

(Promega), 1 μl of 1 mM Methionine (Promega), and 4 μl of nuclease-free water, and the resultant mixture was incubated at 30 °C for 3 h.

Trans cleavage of FCV capsid precursor protein

To examine the cleavage activity of FCV 3C-like protease in *trans*, 20 μl of *in vitro* translation reaction mixture containing the non-radiolabeled protease active or inactive FCV F4 ORF1 polyprotein, a source of the FCV protease, was mixed with 20 μl of *in vitro* translation reaction mixture containing the radiolabeled FCV capsid precursor (native or mutant), and the resultant 40 μl of the mixture in total was incubated at 30 °C for 3 h. Then 8 μl of the reaction mixture was mixed with 20 μl of the SDS–PAGE sample buffer and heated at 95 °C for 5 min, and then 10 μl of the sample was loaded onto 5% to 20% Tris–Gly polyacrylamide gel (D.R.C., Tokyo).

Immunoprecipitation

For the radioimmunoprecipitation assay, 10 μl of the reaction mixture was diluted with 80 μl of RIPA lysis buffer containing 50 mM Tris, pH 7.4, 150 mM NaCl, 0.25% deoxycholic acid, 1% NP40, 1 mM EDTA (Upstate, Lake Placid, NY) and incubated with 5 μg of region-specific antibodies, anti-A or anti-D raised against *E. coli*-expressed recombinant proteins A (aa 1–231) or D (aa 941–1055) (Oka et al., 2005). After incubation for 1 h on ice, 25 μl of a suspension of protein A magnetic beads (New England Biolabs) and 900 μl of RIPA buffer were added. The mixture was gently rotated at 4 °C for 1 h and then washed three times with 1 ml of RIPA lysis buffer. The immunoprecipitated proteins were resuspended in 20 μl of SDS–PAGE sample buffer and heated at 95 °C for 5 min prior to analysis with 5% to 20% Tris–Gly polyacrylamide gel.

Analysis of the translated proteins

The translation products were separated by SDS–PAGE. The proteins in the gel were blotted onto a PVDF membrane (Immobilon-P: Millipore, Bedford, MA) using a semi-dry electroblotting apparatus (ATTO, Tokyo). The radiolabeled proteins were detected by a Bioimage Analyzer BAS 2500 (Fuji Film, Tokyo). A panel of individual mature and intermediate proteins was expressed with the same system and used for identification of the cleavage products generated from the polyprotein.

Nucleotide and amino acid sequence analyses

To confirm the sequences of the panel of plasmids used in this study, nucleotide sequence analysis was performed with the Big Dye Terminator (version 3.1) Cycle Sequencing Ready Reaction Kit (Applied Biosystems, Tokyo, Japan) and an automated sequencer, the 3130 Genetic Analyzer, or an ABI 3730 xl DNA analyzer (Applied Biosystems). Nucleotide sequences were assembled with the program Sequencher™, version 4.7 (Gene Codes Corp., Ann Arbor, MI). Nucleotide and amino acid sequences were analyzed with GENETYX® Mac software, version 12.2.6 (Genetyx Corp., Tokyo, Japan).

Analysis of amino acid variation

A total of 98 sequences of calicivirus full-length ORF1 were collected from a public database (for accession numbers, see Amino acid sequences section). Cleavage site sequences of ORF1s and VP1 precursor proteins of viruses representing each of the four genera of the family *Caliciviridae* ($n=114$, 160, 231, and 84 sequences for SaV, NoV, RHDV, and FCV strains, respectively) were aligned with CLUSTALW Version 1.83 (Thompson et al., 1994).

Amino acid variations at the P1, P2, P3, and P4 positions of the calicivirus precursor cleavage site were calculated as previously described (Motomura et al., 2008; Naganawa et al., 2008) on the basis of Shannon's equation (Shannon, 1997):

$$H(i) = -\sum_{x_i} p(x_i)\log_2 p(x_i) \quad (x_i = G, A, I, V, \ldots\ldots),$$

where $H(i)$, $p(x_i)$, and i indicate the amino acid entropy score of a given position, the probability of occurrence of a given amino acid at the position, and the number of positions, respectively. An $H(i)$ score of zero indicates absolute conservation, whereas a score of 4.4 indicates complete randomness.

We also calculated the Shannon entropy by considering the physicochemical properties of amino acids, i.e., size and chemical properties. In case of size-based variation analysis, amino acids are classified into four groups: small (Gly, Ala, Cys, Ser), medium–small (Thr, Val, Asn, Asp, Ile, Leu, Pro, Met), medium–large (Gln, Glu, Arg, Lys), and large (His, Phe, Tyr, Try).

In case of chemical-property-based variation analysis, amino acids are classified into seven groups: acidic (Asp, Glu), basic (Arg, Lys, His), neutral hydrophilic (Ser, Thr, Asn, Gln), aliphatic (Gly, Ala, Val, Ile, Leu, Met), aromatic (Phe, Tyr, Trp), thio-containing (Cys), and imine (Pro). The entropy scores were calculated on the assumption that the amino acids within the same group are the same amino acid.

Amino acid sequences

The following are the accession numbers for the nucleotide sequences used in the present studies: human SaV strains ($n=19$), AY237420, AY237422, X86560, AY694184, AY237423, AY646853, AY646854, DQ366345, AJ786349, AJ249939, AY603425, AY237419, AY646855, DQ058829, DQ125333, DQ125334, DQ366346, AY646856, and DQ366344; human NoV strains ($n=32$), AB039782, M87661, AB042808, U07611, X86557, L07418, AF145896, AY032605, AB039774, AB039775, AB039776, AB039777, AB039778, AB039779, AB039780, AB039781, AB044366, AB045603, AB081723, AB083780, AB084071, AB187514, AB365435, AF093797, AY134748, AY237415, AY587989, AY741811, DQ093067, DQ366347, DQ456824, and EU310927; RHDV strains ($n=33$), AB300693, AF258618, AY523410, DQ189077, DQ205345, DQ280493, EF363035, NC_001543, U54983, X87607, Z29514, Z49271, EU003578, EU003579, EU003581, EU003582, AF295785, DQ189078, EF558572, EF558573, EF558574, EF558575, EF558576, EF558577, EF558578, EF558579, EF558580, EF558581, EF558582, EF558583, EF558584, EF558585, and EF558586; and FCV strains ($n=14$), D31836, AF109465, AF479590, L40021, M86379, U13992, DQ424892, AY560113, AY560114, AY560115, AY560116, AY560117, AY560118, and NC_001481.

Acknowledgments

This work was supported in part by a Grant-in-Aid for Young Scientists (B) from the Ministry of Education, Culture, Sports, Science and Technology of Japan, a grant from the Japan Health Science Foundation, and grants for Food Safety and For Research on Emerging and Re-emerging Infectious Diseases from the Ministry of Health, Labour, and Welfare of Japan.

Appendix A. Supplementary data

Supplementary data associated with this article can be found, in the online version, at doi:10.1016/j.virol.2009.08.018.

References

Belliot, G., Sosnovtsev, S.V., Mitra, T., Hammer, C., Garfield, M., Green, K.Y., 2003. In vitro proteolytic processing of the MD145 norovirus ORF1 nonstructural polyprotein yields stable precursors and products similar to those detected in calicivirus-infected cells. J. Virol. 77 (20), 10957–10974.

Blair, W.S., Semler, B.L., 1991. Role for the P4 amino acid residue in substrate utilization by the poliovirus 3CD proteinase. J. Virol. 65 (11), 6111–6123.

Blakeney, S.J., Cahill, A., Reilly, P.A., 2003. Processing of Norwalk virus nonstructural proteins by a 3C-like cysteine proteinase. Virology 308 (2), 216–224.

Boniotti, B., Wirblich, C., Sibilia, M., Meyers, G., Thiel, H.J., Rossi, C., 1994. Identification and characterization of a 3C-like protease from rabbit hemorrhagic disease virus, a calicivirus. J. Virol. 68 (10), 6487–6495.

Clarke, I.N., Lambden, P.R., 1997. The molecular biology of caliciviruses. J. Gen. Virol. 78 (Pt 2), 291–301.

Clarke, I.N., Lambden, P.R., 2000. Organization and expression of calicivirus genes. J. Infect. Dis. 181 (Suppl. 2), S309–S316.

Gorchakov, R., Frolova, E., Sawicki, S., Atasheva, S., Sawicki, D., Frol ov, I., 2008. A new role for ns polyprotein cleavage in Sindbis virus replication. J. Virol. 82 (13), 6218–6231.

Green, K.Y., 2007. Caliciviridae: the noroviruses: specific virus families, In: Knipe, D.M., Howley, P.M., Griffin, D.E., Lamb, R.A., Martin, M.A., Roizman, B., Straus, S.E. (Eds.), Fields Virology, 5th ed. Lippincott Williams & Wilkins, Philadelphia, pp. 949–979.

Hansman, G.S., Katayama, K., Maneekarn, N., Peerakome, S., Khamrin, P., Tonusin, S., Okitsu, S., Nishio, O., Takeda, N., Ushijima, H., 2004. Genetic diversity of norovirus and sapovirus in hospitalized infants with sporadic cases of acute gastroenteritis in Chiang Mai, Thailand. J. Clin. Microbiol. 42 (3), 1305–1307.

Hardy, M.E., Crone, T.J., Brower, J.E., Ettayebi, K., 2002. Substrate specificity of the Norwalk virus 3C-like proteinase. Virus Res. 89 (1), 29–39.

Jewell, D.A., Swietnicki, W., Dunn, B.M., Malcolm, B.A., 1992. Hepatitis A virus 3C proteinase substrate specificity. Biochemistry 31 (34), 7862–7869.

Kageyama, T., Shinohara, M., Uchida, K., Fukushi, S., Hoshino, F.B., Kojima, S., Takai, R., Oka, T., Takeda, N., Katayama, K., 2004. Coexistence of multiple genotypes, including newly identified genotypes, in outbreaks of gastroenteritis due to norovirus in Japan. J. Clin. Microbiol. 42 (7), 2988–2995.

Katayama, K., Hansman, G.S., Oka, T., Ogawa, S., Takeda, N., 2006. Investigation of norovirus replication in a human cell line. Arch. Virol. 151 (7), 1291–1308.

Katayama, K., Shirato-Horikoshi, H., Kojima, S., Kageyama, T., Oka, T., Hoshino, F., Fukushi, S., Shinohara, M., Uchida, K., Suzuki, Y., Gojobori, T., Takeda, N., 2002. Phylogenetic analysis of the complete genome of 18 Norwalk-like viruses. Virology 299 (2), 225–239.

Liu, B., Clarke, I.N., Lambden, P.R., 1996. Polyprotein processing in Southampton virus: identification of 3C-like protease cleavage sites by in vitro mutagenesis. J. Virol. 70 (4), 2605–2610.

Makino, A., Shimojima, M., Miyazawa, T., Kato, K., Tohya, Y., Akashi, H., 2006. Junctional adhesion molecule 1 is a functional receptor for feline calicivirus. J. Virol. 80 (9), 4482–4490.

Martin Alonso, J.M., Casais, R., Boga, J.A., Parra, F., 1996. Processing of rabbit hemorrhagic disease virus polyprotein. J. Virol. 70 (2), 1261–1265.

Matsuura, Y., Tohya, Y., Onuma, M., Roerink, F., Mochizuki, M., Sugimura, T., 2000. Expression and processing of the canine calicivirus capsid precursor. J. Gen. Virol. 81 (Pt. 1), 195–199.

Meyers, G., Wirblich, C., Thiel, H.J., Thumfart, J.O., 2000. Rabbit hemorrhagic disease virus: genome organization and polyprotein processing of a calicivirus studied after transient expression of cDNA constructs. Virology 276 (2), 349–363.

Motomura, K., Oka, T., Yokoyama, M., Nakamura, H., Mori, H., Ode, H., Hansman, G.S., Katayama, K., Kanda, T., Tanaka, T., Takeda, N., Sato, H., 2008. Identification of monomorphic and divergent haplotypes in the 2006–2007 norovirus GII/4 epidemic population by genomewide tracing of evolutionary history. J. Virol. 82 (22), 11247–11262.

Naganawa, S., Yokoyama, M., Shiino, T., Suzuki, T., Ishigatsubo, Y., Ueda, A., Shirai, A., Takeno, M., Hayakawa, S., Sato, S., Tochikubo, O., Kiyoura, S., Sawada, K., Ikegami, T., Kanda, T., Kitamura, K., Sato, H., 2008. Net positive charge of HIV-1 CRF01_AE V3 sequence regulates viral sensitivity to humoral immunity. PLoS ONE 3 (9), e3206.

Nakamura, K., Someya, Y., Kumasaka, T., Ueno, G., Yamamoto, M., Sato, T., Takeda, N., Miyamura, T., Tanaka, N., 2005. A norovirus protease structure provides insights into active and substrate binding site integrity. J. Virol. 79 (21), 13685–13693.

Oehmig, A., Buttner, M., Weiland, F., Werz, W., Bergemann, K., Pfaff, E., 2003. Identification of a calicivirus isolate of unknown origin. J. Gen. Virol. 84 (Pt. 10), 2837–2845.

Oka, T., Katayama, K., Ogawa, S., Hansman, G.S., Kageyama, T., Ushijima, H., Miyamura, T., Takeda, N., 2005. Proteolytic processing of sapovirus ORF1 polyprotein. J. Virol. 79 (12), 7283–7290.

Oka, T., Yamamoto, M., Katayama, K., Hansman, G.S., Ogawa, S., Miyamura, T., Takeda, N., 2006. Identification of the cleavage sites of sapovirus open reading frame 1 polyprotein. J. Gen. Virol. 87 (Pt 11), 3329–3338.

Oka, T., Yamamoto, M., Yokoyama, M., Ogawa, S., Hansman, G.S., Katayama, K., Miyashita, K., Takagi, H., Tohya, Y., Sato, H., Takeda, N., 2007. Highly conserved configuration of catalytic amino acid residues among calicivirus-encoded proteases. J. Virol. 81 (13), 6798–6806.

Pallai, P.V., Burkhardt, F., Skoog, M., Schreiner, K., Bax, P., Cohen, K.A., Hansen, G., Palladino, D.E., Harris, K.S., Nicklin, M.J., et al., 1989. Cleavage of synthetic peptides by purified poliovirus 3C proteinase. J. Biol. Chem. 264 (17), 9738–9741.

Pathak, H.B., Oh, H.S., Goodfellow, I.G., Arnold, J.J., Cameron, C.E., 2008. Picornavirus genome replication: roles of precursor proteins and rate-limiting steps in oriI-dependent VPg uridylylation. J. Biol. Chem. 283 (45), 30677–30688.

Pettit, S.C., Moody, M.D., Wehbie, R.S., Kaplan, A.H., Nantermet, P.V., Klein, C.A., Swanstrom, R., 1994. The p2 domain of human immunodeficiency virus type 1 Gag regulates sequential proteolytic processing and is required to produce fully infectious virions. J. Virol. 68 (12), 8017–8027.

Rinehart-Kim, J.E., Zhong, W.M., Jiang, X., Smith, A.W., Matson, D.O., 1999. Complete nucleotide sequence and genomic organization of a primate calicivirus, Pan-1. Arch. Virol. 144 (1), 199–208.

Robel, I., Gebhardt, J., Mesters, J.R., Gorbalenya, A., Coutard, B., Canard, B., Hilgenfeld, R., Rohayem, J., 2008. Functional characterization of the cleavage specificity of the sapovirus chymotrypsin-like protease. J. Virol. 82 (16), 8085–8093.

Schechter, I., Berger, A., 1967. On the size of the active site in proteases. I. Papain. Biochem. Biophys. Res. Commun. 27 (2), 157–162.

Scheffler, U., Rudolph, W., Gebhardt, J., Rohayem, J., 2007. Differential cleavage of the norovirus polyprotein precursor by two active forms of the viral protease. J. Gen. Virol. 88 (Pt. 7), 2013–2018.

Seah, E.L., Marshall, J.A., Wright, P.J., 1999. Open reading frame 1 of the Norwalk-like virus Camberwell: completion of sequence and expression in mammalian cells. J. Virol. 73 (12), 10531–10535.

Seah, E.L., Marshall, J.A., Wright, P.J., 2003. Trans activity of the norovirus Camberwell proteinase and cleavage of the N-terminal protein encoded by ORF1. J. Virol. 77 (12), 7150–7155.

Shannon, C.E., 1997. The mathematical theory of communication. MD. Comput. 14 (4), 306–317.

Sosnovtsev, S.V., Belliot, G., Chang, K.O., Prikhodko, V.G., Thackray, L.B., Wobus, C.E., Karst, S.M., Virgin, H.W., Green, K.Y., 2006. Cleavage map and proteolytic processing of the murine norovirus nonstructural polyprotein in infected cells. J. Virol. 80 (16), 7816–7831.

Sosnovtsev, S.V., Garfield, M., Green, K.Y., 2002. Processing map and essential cleavage sites of the nonstructural polyprotein encoded by ORF1 of the feline calicivirus genome. J. Virol. 76 (14), 7060–7072.

Sosnovtsev, S.V., Sosnovtseva, S.A., Green, K.Y., 1998. Cleavage of the feline calicivirus capsid precursor is mediated by a virus-encoded proteinase. J. Virol. 72 (4), 3051–3059.

Sosnovtseva, S.A., Sosnovtsev, S.V., Green, K.Y., 1999. Mapping of the feline calicivirus proteinase responsible for autocatalytic processing of the nonstructural polyprotein and identification of a stable proteinase-polymerase precursor protein. J. Virol. 73 (8), 6626–6633.

Takahashi, E., Konishi, S., Ogata, M., 1971. Studies on cytopathogenic viruses from cats with respiratory infections. II. Characterization of feline picornaviruses. Nippon Juigaku Zasshi 33 (2), 81–87.

Thompson, J.D., Higgins, D.G., Gibson, T.J., 1994. CLUSTAL W: improving the sensitivity of progressive multiple sequence alignment through sequence weighting, position-specific gap penalties and weight matrix choice. Nucleic Acids Res. 22 (22), 4673–4680.

Wiegers, K., Rutter, G., Kottler, H., Tessmer, U., Hohenberg, H., Krausslich, H.G., 1998. Sequential steps in human immunodeficiency virus particle maturation revealed by alterations of individual Gag polyprotein cleavage sites. J. Virol. 72 (4), 2846–2854.

Wirblich, C., Sibilia, M., Boniotti, M.B., Rossi, C., Thiel, H.J., Meyers, G., 1995. 3C-like protease of rabbit hemorrhagic disease virus: identification of cleavage sites in the ORF1 polyprotein and analysis of cleavage specificity. J. Virol. 69 (11), 7159–7168.

Wirblich, C., Thiel, H.J., Meyers, G., 1996. Genetic map of the calicivirus rabbit hemorrhagic disease virus as deduced from in vitro translation studies. J. Virol. 70 (11), 7974–7983.

Yap, C.C., Ishii, K., Aizaki, H., Tani, H., Aoki, Y., Ueda, Y., Matsuura, Y., Miyamura, T., 1998. Expression of target genes by coinfection with replication-deficient viral vectors. J. Gen. Virol. 79 (Pt. 8), 1879–1888.

Microbiol Immunol 2009; **53**: 49–52
doi:10.1111/j.1348-0421.2008.00086.x

NOTE

Self-assembly of sapovirus recombinant virus-like particles from polyprotein in mammalian cells

Tomoichiro Oka†, Mami Yamamoto†, Kana Miyashita, Satoko Ogawa*, Kazuhiko Katayama, Takaji Wakita and Naokazu Takeda

Department of Virology II, National Institute of Infectious Diseases, Gakuen 4-7-1, Musashi-murayama, Tokyo 208-0011, Japan

ABSTRACT

The SaV genome is a positive-sense, non-segmented single-strand RNA molecule of approximately 7.5 kb that is polyadenylated at its 3′ terminus. The major capsid (VP1) of SaV is thought to be produced as the ORF1 polyprotein followed by cleavage, or translation from subgenomic RNA (3′-coterminal with the virus genome), or both. We have recently reported the formation of SaV VLP from subgenomic-like RNA in mammalian cells. In the present study, we demonstrated that the VP1 cleaved from a part of ORF1 polyprotein self-assembled into VLP in mammalian cells when a transient expression system using a recombinant vaccinia virus encoding T7 RNA polymerase was used.

Key words proteolytic processing, sapovirus, virus-like particle.

The family *Caliciviridae* includes four genera (*Sapovirus* [SaV], *Norovirus*, *Lagovirus* and *Vesivirus*) (1). SaV is a pathogen causing gastroenteritis in humans and pigs (1, 2). Based on the capsid (VP1) gene sequence, SaV strains are divided into five genogroups, GI to GV, of which the GI, GII, GIV and GV strains infect humans, while the GIII strains infect swine (3). Only the GIII strains can be propagated in cultured cells (4). The SaV genome is a positive-sense, non-segmented single-strand RNA molecule of approximately 7.5 kb that is polyadenylated at its 3′ terminus. The SaV genomes are predicted to encode two or three ORF. The SaV ORF1 encodes non-structural proteins and a single structural protein, whereas the functions of ORF2- and ORF3-encoded proteins are still unknown (5, 6). ORF3 is only found in GI, GIV and GV SaV strains (3, 7–9). "NH_2-p11-p28-p35(NTPase)-p32-p14(VPg)-p70(ProPol)-p60(VP1)-COOH" is the SaV GII Mc10 ORF1 polyprotein cleavage map (Fig. 1) (10). Mutagenesis of the GDCG motif in the 3C-like protease fully abolished the proteolytic activity, demonstrating that the cleavage was dependent on a virally encoded 3C-like protease (10–13). p70 (ProPol) has two aa motifs characteristic of Pro and Pol; however, we were unable to demonstrate further processing between Pro and Pol in either an *in vitro* rabbit reticulocyte-coupled transcription-translation system or in an *Escherichia coli* expression system (10–13). The major capsid (VP1) gene of SaV is encoded on ORF1 and fused to the non-structural genes, whereas the subgenomic RNA (likely the 3′-coterminal with the virus genome) was recently identified in cells infected with a GIII SaV strain (4). A tripeptide, MEG or MEA, conserved among human SaV strains or porcine SaV strains, (8, 9) is likely to be the putative VP1 start on the subgenomic RNA. We have recently identified the cleavage site between ProPol and VP1 as ME^{1722}/G^{1723} within the conserved tripeptides (13). Therefore, the VP1 may be produced by either translation as part of the ORF1 polyprotein followed by cleavage, or translation from subgenomic RNA, or by

Correspondence
Tomoichiro Oka, Department of Virology II, National Institute of Infectious Diseases, Gakuen 4-7-1, Musashi-murayama, Tokyo 208-0011, Japan.
Tel: +81 42 561 0771; fax: +81 42 561 4729; email: oka-t@nih.go.jp

***Present Address**
Mitsubishi Kagaku Institute of Life Sciences, Minamiooya 11, Machida, Tokyo 194-8511, Japan.

†These authors contributed equally to this study.

Received 23 July 2008; revised 2 August 2008; accepted 8 August 2008.

List of Abbreviations: ORF, open reading frame; SaV, sapovirus; VLP, virus-like particles.

© 2009 The Societies and Blackwell Publishing Asia Pty Ltd

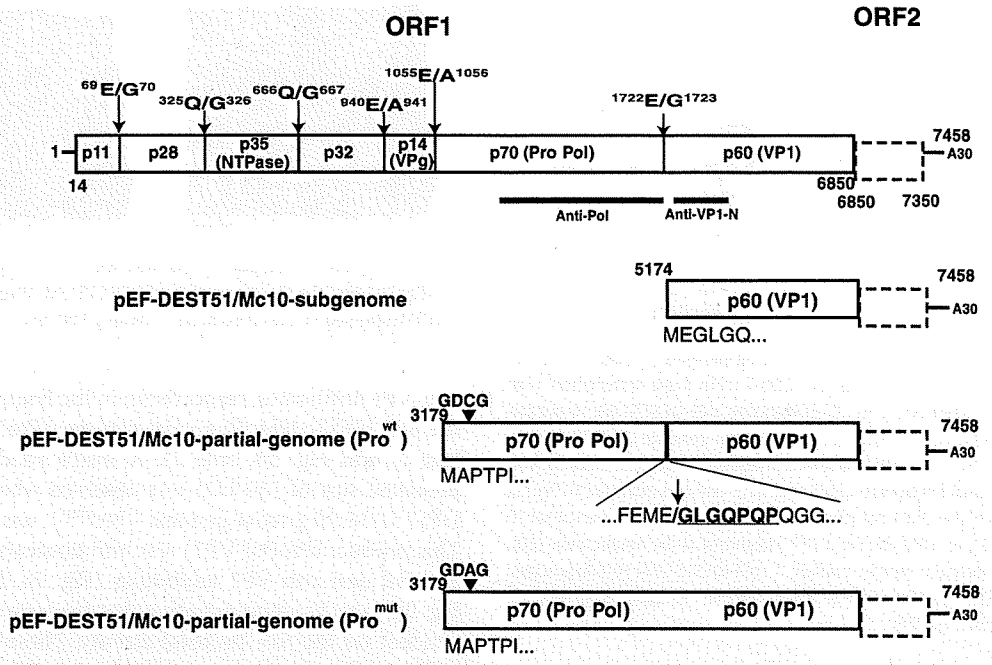

Fig. 1. Diagram of the genome and cleavage maps of the Mc10 ORF1 polyprotein and schematic representation of the proteins expressed in COS-7 cells. The subgenomic and partial genomic regions were cloned into the pEF/DEST vector and designated as the pEF-DEST51/Mc10-subgenome, pEF-DEST51/Mc10-partial-genome (Pro^{wt}) and pEF-DEST51/ Mc10-partial-genome (Pro^{mut}), respectively. The closed triangle indicates the position in the 3C-like protease where the C-to-A change in the GDCG motif was introduced. The cleavage site identified in the translated product from the pEF-DEST51/Mc10-partial-genome (Pro^{wt}) is indicated by a forward slash and arrow.

both, as reported in another member of calicivirus, the rabbit hemorrhagic disease virus from the genus *Lagovirus* (14). The VP1 expressed from the putative subgenomic RNA construct self-assembled into VLP, which are morphologically similar to native SaV, in insect (15–22) or mammalian cells (23), whereas it remains unclear whether VLP are assembled from autocatalytically processed VP1 from the ORF1 polyprotein. The objectives of the present study were to determine whether VLP formation occurs when a partial ORF1 polyprotein is expressed in mammalian cells, and whether the putative p70 (ProPol) region of human SaV is further cleaved in mammalian cells.

To construct the Mc10 expression plasmids, DNA fragments corresponding to the putative subgenomic region (nt 5174–7458: GenBank Accession No. AY237420) or the partial genomic region from the protease to the genome end (nt 3179–7458) with or without nucleotide changes from TGT (^{1171}C) to GCG (^{1171}A) in the GDCG motif of the protease were amplified by PCR with pUC19/SaV Mc10 full-length and pUC19/SaV Mc10 full-C1171A/ORF1, the latter of which contains a ^{1169}GDCG^{1172} to GDAG mutation in the protease (10) as templates. PCR was carried out in 100 μL reaction mixture containing 100 ng plasmid, 40 pmol of each primer, 10 μL KOD polymerase buffer, 0.2 mM of each dNTP, 1 mM $MgSO_4$, and 2 U of KOD-Plus-DNA polymerase (Toyobo, Osaka, Japan). After initial denaturation at 94 °C for 10 min, 25 cycles consisting of denaturation at 94 °C for 30 s, primer annealing at 55 °C for 30 s, and primer extension at 72 °C for 5 min were carried out, followed by a final extension at 72 °C for 15 min. The PCR products were purified using a QIAquick PCR Purification Kit (Qiagen, Tokyo, Japan) and cloned into the pEF-DEST51 vector (Invitrogen Japan, Tokyo, Japan) harboring both the human elongation factor 1α and T7 promoter with the Gateway Cloning System (Invitrogen) according to the manufacturer's protocol. The resulting plasmids were designated as the pEF-DEST51/Mc10-subgenome, pEF-DEST51/Mc10-partial-genome (Pro^{wt}) and pEF-DEST51/Mc10-partial-genome (Pro^{mut}), respectively (Fig. 1). The designation 'Pro^{mut}' refers to a protease in which C was changed to A in the GDCG motif as described previously (10–13). *E. coli* DH5α cells (Toyobo) were used for the transformation and propagation of the plasmid.

COS-7 cells grown in six-well culture plates (BD Falcon, Franklin Lakes, NJ, USA) were infected with a

© 2009 The Societies and Blackwell Publishing Asia Pty Ltd

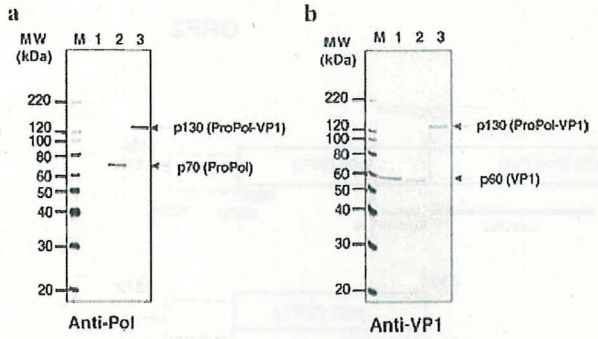

Fig. 2. Western blot analysis of translated proteins in COS-7 cells. Recombinant vaccinia virus-infected COS-7 cells were transfected with the plasmid (pEF-DEST51/Mc10-subgenome, pEF-DEST51/Mc10-partial-genome [Pro^{wt}] or pEF-DEST51/ Mc10-partial-genome [Pro^{mut}]) and incubated for 48 hr. The cell lysate was analyzed by western blotting with rabbit polyclonal antibodies raised against *E. coli*-expressed Mc10 Pol (aa 1247–1720 of the ORF1 polyprotein) (a) and the N-terminal part of Mc10 VP1 (aa 1721 to 1950 of the ORF1 polyprotein) (b), respectively (10). Lanes: M, molecular weight marker; 1, pEF-DEST51/Mc10-subgenome; 2, pEF-DEST51/Mc10-partial-genome (Pro^{wt}); 3, pEF-DEST51/Mc10-partial-genome (Pro^{mut}).

recombinant vaccinia virus which expresses the T7 RNA polymerase (24) at a multiplicity of infection (MOI) of 1, and incubated at 37 °C for 1 hr. Then, the plasmid pEF-DEST51/Mc10-subgenome, pEF-DEST51/Mc10-partial-genome (Pro^{wt}) or pEF-DEST51/ Mc10-partial-genome (Pro^{mut}), 2 μg per well, was transfected into the COS-7 cells using FuGENE HD Transfection Reagent (Roche, Mannheim, Germany) according to the manufacturer's protocol. The cells were incubated at 37 °C for 48 hr, and the medium was removed. The cells were collected by scraping with 300 μL/well of OPTI-MEM (Invitrogen). For western blotting, the proteins separated in the SDS-PAGE were electrically blotted onto a PVDF membrane (Immobilon-P; Millipore, Billerica, MA, USA) and detected with anti-Pol and -VP1 rabbit hyperimmune IgG (10) at a dilution of 1:3000 as previously described (12, 23). The membrane was treated with ECL detection reagent (GE Healthcare Biosciences, Uppsala, Sweden) according to the manufacturer's instructions, and the signals were detected with an LAS3000 Imaging system (Fuji Film, Tokyo, Japan). Magicmark XP Western standard (Invitrogen) was used as a size marker for the western blotting.

When the total lysate of mammalian cells expressing the pEF-DEST51/Mc10-subgenome was analyzed by western blotting, a single major protein of approximately 60 kDa was visualized with anti-VP1 antibodies (Fig. 2b, lane 1), and no signal was detected with anti-Pol (Fig. 2a, lane 1). In contrast, two major proteins of approximately 70 kDa and 60 kDa were visualized with anti-Pol and anti-VP1 antibodies, respectively, in the lysate expressing the pEF-DEST51/Mc10-partial-genome (Pro^{wt}) (Fig. 2a, lane 2, and Fig. 2b, lane 2). A major product with a predicted size of 130 kDa was observed when the pEF-DEST51/Mc10-partial-genome (Pro^{mut}) was expressed. This product (ProPol-VP1) was immunoreactive to both anti-Pol and anti-VP1 antibodies (Fig. 2a, lane 3, and Fig. 2b, lane 3), demonstrating that the cleavage was dependent on the SaV protease activity. These results also indicated that the cleavage within ProPol did not occur in mammalian cells, which was in agreement with our previous findings in both an *in vitro* transcription/translation system and in an *E. coli* expression system (10–13). The size of the VP1 derived from the partial ORF1 polyprotein was slightly smaller than that derived from the subgenomic construct when analyzed by SDS-PAGE (Fig. 2b, lanes 1 and 2).

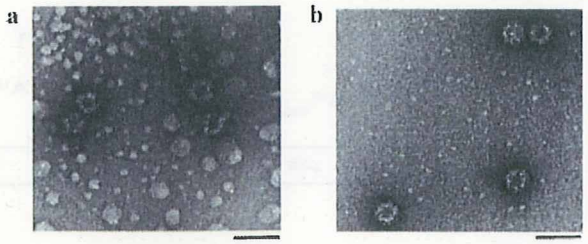

Fig. 3. Electron micrograph of purified Mc10 VLP derived from (a) pEF-DEST51/Mc10-subgenome or (b) pEF-DEST51/Mc10-partial-genome (Pro^{wt}) expressed in COS-7 cells. Bar indicates 100 nm.

To determine whether VLP were generated or not, the cell suspension (collected from 10 six-well plates) was subjected to three cycles of freezing and thawing, and the cell debris was removed by centrifugation (2300 $\times g$, 5 min at 4 °C). VLP from the cell lysate were pelleted by centrifugation in a Beckman Coulter (Tokyo, Japan) SW32-Ti rotor (r max 164 000$\times g$, 2 hr at 10 °C) and resuspended in 500 μL OPTI-MEM at 4 °C, and the debris was removed by low-speed centrifugation (2300 $\times g$, 5 min at 4 °C). The supernatant was further separated by 5–30% (wt/vol) sucrose density gradient centrifugation in a Beckman Coulter SW41 rotor at r max 107 000$\times g$ for 2.5 hr at 10 °C. After fractionation (24 $\times$ 500 μL each), each aliquot was centrifuged at r max 125 000$\times g$ for 3 hr at 4 °C in a Beckman Coulter TLA55 rotor. The resulting pellet was resuspended in 20 μL OPTI-MEM. Western blotting of each fraction with anti-VP1 antibodies revealed that a single major protein of approximately 60 kDa appeared in similar fractions (20.5–19.9% [wt/vol] in the case of the pEF-DEST51/Mc10-subgenome and 21.3–19.5% [wt/vol] in the case of the pEF-DEST51/Mc10-partial-genome [Pro^{wt}]) (data not shown). The peak fractions containing 60 kDa protein were subjected to electron microscopy

© 2009 The Societies and Blackwell Publishing Asia Pty Ltd

and N-terminal amino acid sequencing (APRO Science, Tokushima, Japan). Electron microscopy analysis showed that both constructs generated morphologically similar VLP approximately 40–45 nm in diameter (Fig. 3a,b). The N-terminal amino acid sequence of the 60 kDa protein from the pEF-DEST51/Mc10-partial-genome (Pro^{wt}) was GLGQPQP, which corresponds to SaV Mc10 ORF1 aa 1723–1729 (Fig. 1). These results demonstrated that efficient cleavage occurred at the recently identified site (between E^{1722} and G^{1723}) *in vitro* (13), and the cleaved VP1 self-assembled into VLP. An attempt to identify the N-terminal amino acid sequence of the major 60 kDa protein in the VLP peak fraction from pEF-DEST51/Mc10-subgenome failed, probably because of N-terminus blocking (data not shown). The size of the VP1 derived from the partial ORF1 polyprotein is smaller than that derived from the subgenomic construct in SDS-PAGE (Fig. 2b, lanes 1 and 2), which is likely to be due to two amino acids truncation in the VP1 derived from the partial ORF1 polyprotein and/or the presence of an additional molecule at the N-terminus of the VP1 derived from the subgenomic construct.

In conclusion, our results demonstrated the following: (i) no cleavage occurred within the ProPol protein; (ii) efficient cleavage occurred at the E^{1722} and G^{1723} site between p70 (ProPol) and p60 (VP1) in mammalian cells; (iii) C^{1171} was critical for this cleavage activity; and (iv) cleaved VP1 derived from a partial ORF1 polyprotein self-assembled into VLP morphologically similar to those derived from the subgenomic-like construct.

ACKNOWLEDGMENTS

We thank Dr B. Moss for providing the recombinant vaccinia virus encoding T7 RNA polymerase and G. S. Hansman for his technical support. This work was supported in part by a grant for Research on Food Safety from the Ministry of Health, Labour and Welfare of Japan, and a grant from The Japan Health Science Foundation.

REFERENCES

1. Mayo M.A. (2002) A summary of taxonomic changes recently approved by ICTV. *Arch Virol* **147:** 1655–63.
2. Hansman G.S., Oka T., Katayama K., Takeda N. (2007) Human sapoviruses: genetic diversity, recombination, and classification. *Rev Med Virol* **17:** 133–41.
3. Farkas T., Zhong W.M., Jing Y., Huang P.W., Espinosa S.M., Martinez N. *et al.* (2004) Genetic diversity among sapoviruses. *Arch Virol* **149:** 1309–23.
4. Chang K.O., Sosnovtsev S.V., Belliot G., Kim Y., Saif L.J., Green K.Y. (2004) Bile acids are essential for porcine enteric calicivirus replication in association with down-regulation of signal transducer and activator of transcription 1. *Proc Natl Acad Sci USA* **101:** 8733–8.
5. Clarke I.N., Lambden P.R. (2000) Organization and expression of calicivirus genes. *J Infect Dis* **181**(Suppl 2): S309–16.
6. Green K.Y., Ando T., Balayan M.S., Berke T., Clarke I.N., Estes M.K. *et al.* (2000) Taxonomy of the caliciviruses. *J Infect Dis* **181**(Suppl 2): S322–30.
7. Guo M., Chang K.O., Hardy M.E., Zhang Q., Parwani A.V., Saif L.J. (1999) Molecular characterization of a porcine enteric calicivirus genetically related to Sapporo-like human caliciviruses. *J Virol* **73:** 9625–31.
8. Schuffenecker I., Ando T., Thouvenot D., Lina B., Aymard M. (2001) Genetic classification of "Sapporo-like viruses". *Arch Virol* **146:** 2115–32.
9. Okada M., Yamashita Y., Oseto M., Ogawa T., Kaiho I., Shinozaki K. (2006) Genetic variability in the sapovirus capsid protein. *Virus Genes* **33:** 157–61.
10. Oka T., Katayama K., Ogawa S., Hansman G.S., Kageyama T., Ushijima H. *et al.* (2005) Proteolytic processing of sapovirus ORF1 polyprotein. *J Virol* **79:** 7283–90.
11. Oka T., Yamamoto M., Yokoyama M., Ogawa S., Hansman G.S., Katayama K. *et al.* (2007) Highly conserved configuration of catalytic amino acid residues among calicivirus-encoded proteases. *J Virol* **81:** 6798–806.
12. Oka T., Katayama K., Ogawa S., Hansman G.S., Kageyama T., Miyamura T. *et al.* (2005) Cleavage activity of the sapovirus 3C-like protease in Escherichia coli. *Arch Virol* **150:** 2539–48.
13. Oka T., Yamamoto M., Katayama K., Hansman G.S., Ogawa S., Miyamura T. *et al.* (2006) Identification of the cleavage sites of sapovirus open reading frame 1 polyprotein. *J Gen Virol* **87:** 3329–38.
14. Sibilia M., Boniotti M.B., Angoscini P., Capucci L., Rossi C. (1995) Two independent pathways of expression lead to self-assembly of the rabbit hemorrhagic disease virus capsid protein. *J Virol* **69:** 5812–5.
15. Numata K., Hardy M.E., Nakata S., Chiba S., Estes M.K. (1997) Molecular characterization of morphologically typical human calicivirus Sapporo. *Arch Virol* **142:** 1537–52.
16. Jiang X., Zhong W., Kaplan M., Pickering L.K., Matson D.O. (1999) Expression and characterization of Sapporo-like human calicivirus capsid proteins in baculovirus. *J Virol Methods* **78:** 81–91.
17. Chen R., Neill J.D., Noel J.S., Hutson A.M., Glass R.I., Estes M.K. *et al.* (2004) Inter- and intragenus structural variations in caliciviruses and their functional implications. *J Virol* **78:** 6469–79.
18. Hansman G.S., Katayama K., Oka T., Natori K., Takeda N. (2005) Mutational study of sapovirus expression in insect cells. *Virol J* **2:** 13.
19. Hansman G.S., Matsubara N., Oka T., Ogawa S., Natori K., Takeda N. *et al.* (2005) Deletion analysis of the sapovirus VP1 gene for the assembly of virus-like particles. *Arch Virol* **150:** 2529–38.
20. Hansman G.S., Natori K., Oka T., Ogawa S., Tanaka K., Nagata N. *et al.* (2005) Cross-reactivity among sapovirus recombinant capsid proteins. *Arch Virol* **150:** 21–36.
21. Hansman G.S., Oka T., Katayama K., Takeda N. (2006) Enhancement of sapovirus recombinant capsid protein expression in insect cells. *FEBS Lett* **580:** 4047–50.
22. Hansman G.S., Oka T., Sakon N., Takeda N. (2007) Antigenic diversity of human sapoviruses. *Emerg Infect Dis* **13:** 1519–25.
23. Oka T., Hansman G.S., Katayama K., Ogawa S., Nagata N., Miyamura T. *et al.* (2006) Expression of sapovirus virus-like particles in mammalian cells. *Arch Virol* **151:** 399–404.
24. Fuerst T.R., Niles E.G., Studier F.W., Moss B. (1986) Eukaryotic transient-expression system based on recombinant vaccinia virus that synthesizes bacteriophage T7 RNA polymerase. *Proc Natl Acad Sci USA* **83:** 8122–6.

© 2009 The Societies and Blackwell Publishing Asia Pty Ltd

Jpn. J. Infect. Dis., 61, 2008

Laboratory and Epidemiology Communications

Characterization of Sapoviruses Detected in Hokkaido, Japan

Setsuko Ishida, Shima Yoshizumi, Masahiro Miyoshi, Tetsuya Ikeda, Toyo Okui, Kazuhiko Katayama[1], Naokazu Takeda[1] and Tomoichiro Oka[1]*

Division of Enteric Virology, Department of Microbiology, Hokkaido Institute of Public Health, Sapporo 060-0819, and [1]Department of Virology II, National Institute of Infectious Diseases, Tokyo 208-0011, Japan

Communicated by Takaji Wakita

(Accepted September 16, 2008)

Sapovirus (SaV) is an important pathogen of acute gastroenteritis that often occurs among young children. The SaV prototype strain was detected for the first time in an outbreak in Sapporo, Hokkaido, Japan, in 1977 (1). The SaV genome is a polyadenylated, single-stranded, positive-sense RNA approximately 7.5 kb long, and it has two or three open reading frames (ORFs). ORF1 encodes nonstructural proteins including protease and polymerase and a major structural (capsid) protein, VP1. ORF2 encodes a putative protein with an unknown function. SaV can be divided into five genogroups (GI to GV) based on the capsid protein gene sequences, among which GI, GII, GIV, and GV are known to infect humans, whereas GIII infects porcine species. An additional ORF, overlapping with the 5′ end of the capsid gene, is found in the strains belonging to GI, GIV, and GV (2,3). Human SaV strains are noncultivable, and the most widely used method to detect SaV is reverse-transcription polymerase chain reaction (RT-PCR), which can be used for genetic analysis (4-8). Real-time RT-PCR for SaV was recently developed (9).

The purposes of this study were: (i) to analyze a gastroenteritis outbreak at a health care center for disabled people in 2007 in Kushiro, Hokkaido, Japan, and (ii) to determine the complete capsid sequences of the 2007 strain in comparison with two previously identified strains detected in outbreaks in 2000 in Yakumo and in 2005 in Nayoro, Hokkaido (10).

The outbreak occurred between May 18 and 22 in 2007 in Kushiro, and 10 people (9 adult students and 1 staff member, ages 17-36 years old) developed symptoms of gastroenteritis. During the outbreak, stool specimens were collected from 5 adult students (ages 17-28). These specimens were initially screened for norovirus and group A and group C rotaviruses, but were all found to be negative (data not shown). These 5 specimens were then re-examined for SaV using RT-PCR targeting the polymerase gene with the primers Sapp36 and SV-r-c (4); 4 of the 5 specimens were found to be positive for SaV. To confirm the RT-PCR result and determine the copy number of the SaV genome in the stool specimens, real-time RT-PCR targeting the junction region between the polymerase and capsid was performed (9). All 5 specimens were positive, and the number of cDNA copies per gram of stool ranged between 5.21×10^6 and 2.94×10^9. Sequence analysis revealed that all of the strains belonged to SaV GII, and identical nucleotide sequences were observed in all of the strains (data not shown), indicating that this outbreak was caused by a single GII SaV strain (Kushiro5/2007/JP strain). The specimen that had the highest fecal viral load was subjected to further sequence analysis targeting the partial polymerase, capsid VP1, ORF2, and the 3′ untranslated region of the genome. The 3′ terminus 3.2 kb of the genome was amplified by semi-nested RT-PCR with the forward primer Kushiro PolF1 (5′-GGT TGA GGT GCT CAA TGA ATC-3′) and the reverse primer TX30SXN (5′-GAC TAG TTC TAG ATC GCG AGC GGC CGC CCT TTT TTT TTT TTT TTT TTT TTT TTT TT-3′) for the first PCR, and the forward primer Kushiro PolF2 (5′-GGT ACT TTA CTG CCT TGA CTA C-3′) and TX30SXN for the second PCR. A final volume of 100 μl of reaction mixture containing 2 μl of the cDNA or the first PCR reaction mixture, 10 μl of 10 × KOD-Plus DNA polymerase buffer, 10 μl of 2.5 mM dNTPs, 4 μl of 25 mM $MgSO_4$, 2.5 μl of dimethylsulphoxide (Sigma, St. Louis, Mo., USA), 2 μl of primers (20 pmol/μl each), and 2 μl of KOD-Plus DNA polymerase (1U/μl) (Toyobo, Osaka, Japan), was subjected to PCR at 94°C for 10 min followed by 35 cycles of 94°C for 30 s, 55°C for 30 s, 68°C for 5 min, and a final extension at 72°C for 15 min. The mixture was then held at 4°C. The PCR products were separated with 1% agarose gel electrophoresis, purified with the QIAquick Gel Extraction Kit (Qiagen, Tokyo, Japan), and directly sequenced by a 3130 genetic analyzer (Applied Biosystems, Tokyo, Japan) with the Big Dye Terminator (version 3.1) cycle sequencing kit (Applied Biosystems). Nucleotide sequences were assembled with SEQUENCHER version 4.7 (Gene Codes Corp., Ann Arbor, Mich., USA) and aligned with Clustal

*Corresponding author: Mailing address: Department of Virology II, National Institute of Infectious Diseases, Gakuen 4-7-1, Musashi-murayama, Tokyo 208-0011, Japan. E-mail: oka-t@nih.go.jp